

Adhesive tapes: From daily necessities to flexible smart electronics

Cite as: Appl. Phys. Rev. **10**, 011305 (2023); doi: [10.1063/5.0107318](https://doi.org/10.1063/5.0107318)

Submitted: 4 July 2022 · Accepted: 19 December 2022 ·

Published Online: 23 January 2023



View Online



Export Citation



CrossMark

Xuecheng He,^{1,2}  Wenyu Wang,³  Shijie Yang,²  Feilong Zhang,⁴  Zhen Gu,² Bing Dai,¹ Tailin Xu,^{1,a)} 
Yan Yan Shery Huang,³  and Xueji Zhang^{1,a)}

AFFILIATIONS

¹School of Biomedical Engineering, Health Science Center, Shenzhen University, Shenzhen 518060, China

²Beijing Advanced Innovation Center for Materials Genome Engineering, Research Center for Bioengineering and Sensing Technology, University of Science and Technology Beijing, Beijing 100083, China

³Department of Engineering, University of Cambridge, Cambridge CB2 1PZ, United Kingdom

⁴Innovative Center for Flexible Devices (iFLEX), Max Planck-NTU Joint Lab for Artificial Senses, School of Materials Science and Engineering, Nanyang Technological University, Singapore 639798, Singapore

Note: This paper is part of the special collection on Flexible and Smart Electronics.

^{a)}Authors to whom correspondence should be addressed: xutailin@szu.edu.cn and zhangxueji@szu.edu.cn

ABSTRACT

Imprinting “sticky” features on the surfaces of common non-sticky flexible materials, such as paper, textile, and polymeric films produces a myriad of adhesive tapes that we use in our daily lives. Recently, the rise of flexible electronics has harnessed the distinct adhesive behavior of adhesive tapes to achieve special scientific and engineering purposes. In this review, recent advances including the structures, properties, mechanisms, and functionalities of adhesive tapes and relevant flexible smart electronics are summarized. We provide a key focus on how the distinct adhesive behavior of adhesive tapes contributes to the redesign and engineering of flexible electronics via physical and/or chemical modifications. The applications of these flexible smart electronics enabled by adhesive tapes are widespread, including high-performance sensors, energy storage/conversion devices, medical and healthcare patches, etc. Finally, we discuss unmet needs and current challenges in the development of adhesive tape-enabled materials and techniques for flexible electronics. With ongoing material and technical innovations, adhesive tape-related electronic products are expected to revolutionize our lifestyle and lead us into the era of artificial intelligence.

Published under an exclusive license by AIP Publishing. <https://doi.org/10.1063/5.0107318>

TABLE OF CONTENTS

I. INTRODUCTION	1	IV. ADHESIVE TAPE-ASSISTED MATERIALS AND DEVICES	7
II. GENERAL STRUCTURES AND PROPERTIES OF PRESSURE-SENSITIVE ADHESIVE (PSA) TAPES.	2	A. Physically-dominated techniques	7
A. General structures and properties	2	1. Triboelectrification	7
B. Adhesive mechanism	2	2. Mechanical exfoliation	9
III. COMMON ADHESIVE TAPES USED IN FLEXIBLE ELECTRONICS	4	3. Transfer printing	11
A. Scotch [®] tape series	4	4. Selective removal	12
B. Kapton [®] tape series	6	5. Swab sampling	13
C. Conductive tape	6	6. Stretch-release	14
D. Medical tape	6	7. Bonding	16
E. Tattoo	6	8. Additive techniques	17
F. Elastic tape	7	9. Subtractive techniques	19
G. Stimuli-responsive tape	7	B. Chemically-dominated techniques	19
		1. Mechanochemical activation	19
		2. Chemical deposition	20
		V. OUTLOOK AND CONCLUSION	21

I. INTRODUCTION

In 1930, a young banjo player-turned-3M™ engineer named Richard Drew¹ successfully developed a lightweight, transparent adhesive tape, and then he patented it in the United Kingdom and the United States. Not long after Drew's invention, these adhesive tapes helped people “make do” during the Great Depression—ranging from repairing clothes to protecting broken eggs.¹ Today, almost a hundred years later, flexible electronics as a user-friendly platform have become a hot research area due to their huge potential in transferring traditional bulk and rigid electronics to miniature, low-stiffness, and on-body devices.^{2,3} These flexible electronics are increasingly focused on connecting various items for efficient data collection, transition, and exchange, ultimately facilitating the Internet of Everything. Impressively, the footprint of adhesive tapes has explosively expanded from daily necessities to scientific research beyond one's imagination. The core value of adhesive tapes in the flexible electronics field is their unique adhesive behavior, which enables electronic materials (such as carbon, metal, conductive polymers, and their derivatives) to be either fabricated or introduced onto the tapes with desirable affinity. Today, almost a century after Drew's initial invention, these flexible electronics related to adhesive tapes have motivated extensive applications, such as artificial electronic skin,^{4,5} human-machine interfaces,^{6,7} personalized medicine,^{8,9} wearable sensors,^{10–12} and portable energy generator,^{13,14} etc., which have emphatically changed our lifestyles. These flexible electronics enabled by adhesive tapes, combined with raising information science and technology (5G, big data, Internet of Things, etc.), have brought us into the artificial intelligence era.

In general, the main roles of adhesive tapes in flexible electronics can be summarized into two aspects: one role is passively used as supporting substrates of flexible electronics. When regarded as an adhesive substrate, flexible electronics can be readily produced on adhesive tape using physical and chemical fabrication techniques involving ink-jet printing,¹⁵ screen printing,¹⁶ magnetron sputtering,¹⁷ laser cutting,¹⁸ electrodeposition,^{19,20} etc. Another role of adhesive tapes is to actively construct functional components of flexible electronics. Compared to non-sticky flexible materials fibers,²¹ plastic films,²² and paper,^{23,24} adhesive force is the most significant feature of adhesive tapes. With this key capability in mind, scientists have begun to use adhesive tapes, not simply as substrates, but also to fabricate functional components capable of performing sensing, therapy, or energy-related functions. Regarding the specific mechanism, these approaches include mechanical exfoliation,²⁵ transfer printing,²⁶ stretch-release,⁶ mechanochemical activation,²⁷ etc. For example, the mechanical exfoliation of graphene flakes from bulk graphite using Scotch tape has contributed to the facile fabrication of graphene (Nobel Prize in Physics in 2010) and revolutionized the fabrication techniques of single/few-layer two-dimensional materials (2DMs).²⁵ Some conductive tapes (e.g., conductive carbon and metallic tape) can be directly used as electrodes or contact components.^{28,29} As adhesive tapes are commercially available items, these functional components derived from adhesive tapes have huge potential for rapid translation of flexible devices from the research lab to the medical or consumer market.

The objective of this work is to review current advances in adhesive tape-enabled flexible smart electronics. This review starts with the general structures, properties, and adhesive mechanisms of adhesive tapes. Then, we will categorize common adhesive tapes and their corresponding application scenarios for flexible electronics. By

summarizing the functional electronic materials made by adhesive behavior, or introduced as an additive layer onto adhesive tapes, we attempt to cover the applications of the flexible electronics enabled by adhesive tapes (Fig. 1). Finally, regarding current limitations, the existing challenges, as well as future opportunities for adhesive tape-related flexible electronics will be given.

II. GENERAL STRUCTURES AND PROPERTIES OF PRESSURE-SENSITIVE ADHESIVE (PSA) TAPES

Sometimes, the term “adhesive tape” represents a broader meaning, including polymer patch,³⁹ hydrogel,⁴⁰ biomass-derived fibrin,⁴¹ silk-based adhesives,⁴² etc. These adhesive materials feature intrinsic adhesion and stretchability, which are appealing candidates for flexible healthcare electronics. To enhance the adhesion on complex or biofluid-related interfaces, scientists have already constructed sophisticated micro-nano architectures on these adhesive tapes inspired by the adhesive organs of gecko,⁴³ beetle,⁴⁴ octopus,^{45,46} which can generate physical cross-link, van der Waals (VdWs) force, or cavity-pressure induced adhesion between the substrate and adhesives. Imposing external stimuli can further mediate the adhesion effect.⁴⁷ It is worth noting that these self-design adhesive materials are not the focus of this paper. Instead, the term adhesive tapes in this review refers to off-the-shelf commodities with a clear commercial brand. In this section we will give the structures, properties, and adhesive mechanisms of these well-defined adhesive tapes.

A. General structures and properties

In general, pressure-sensitive adhesive tape is composed of two major compositions, viz., non-sticky backings and sticky adhesives [Fig. 2(a)]. The non-sticky backings are usually made of polymeric film, nonwovens, paper, textiles, metal foil, etc., serving as a physical supporting matrix. The sticky adhesives used in most commercial adhesive tapes are pressure-sensitive adhesives (PSAs, we mainly focus on PSA-type adhesive tapes in this paper), which dominate the adhesive behavior.⁴⁸ The PSAs are aggressive and permanently tacky, capable of being adhered to different adherents (substrates) under slight pressure (no more than finger or hand pressure) in a short period (a few seconds), without the need for activation by heat, solvent, or water, and exert a strong holding force for bonding.⁴⁹ PSAs are a kind of viscoelastic polymer, which can be categorized into acrylics, silicones, polyurethanes (PUs), and epoxies according to the chemical components.⁴⁸

B. Adhesive mechanism

To demonstrate the adhesive mechanism, we start with the required force (P , at an angle of 180°) to peel a PSA material from a rigid substrate, which can be given at the molecular level⁵⁰

$$P = kbl \frac{\pi N_a D \tau}{k_B T} \sigma_b^2,$$

where b and l indicate the width and thickness of the PSA film, respectively, k is a constant related to the contribution of a backing deformation and the interaction between the PSA and substrate, N_a denotes the number of segments of size a in a polymer chain, D is the self-diffusion coefficient of a polymer segment, τ is apparent relaxation time of the adhesive polymer, σ_b represents the ultimate tensile stress

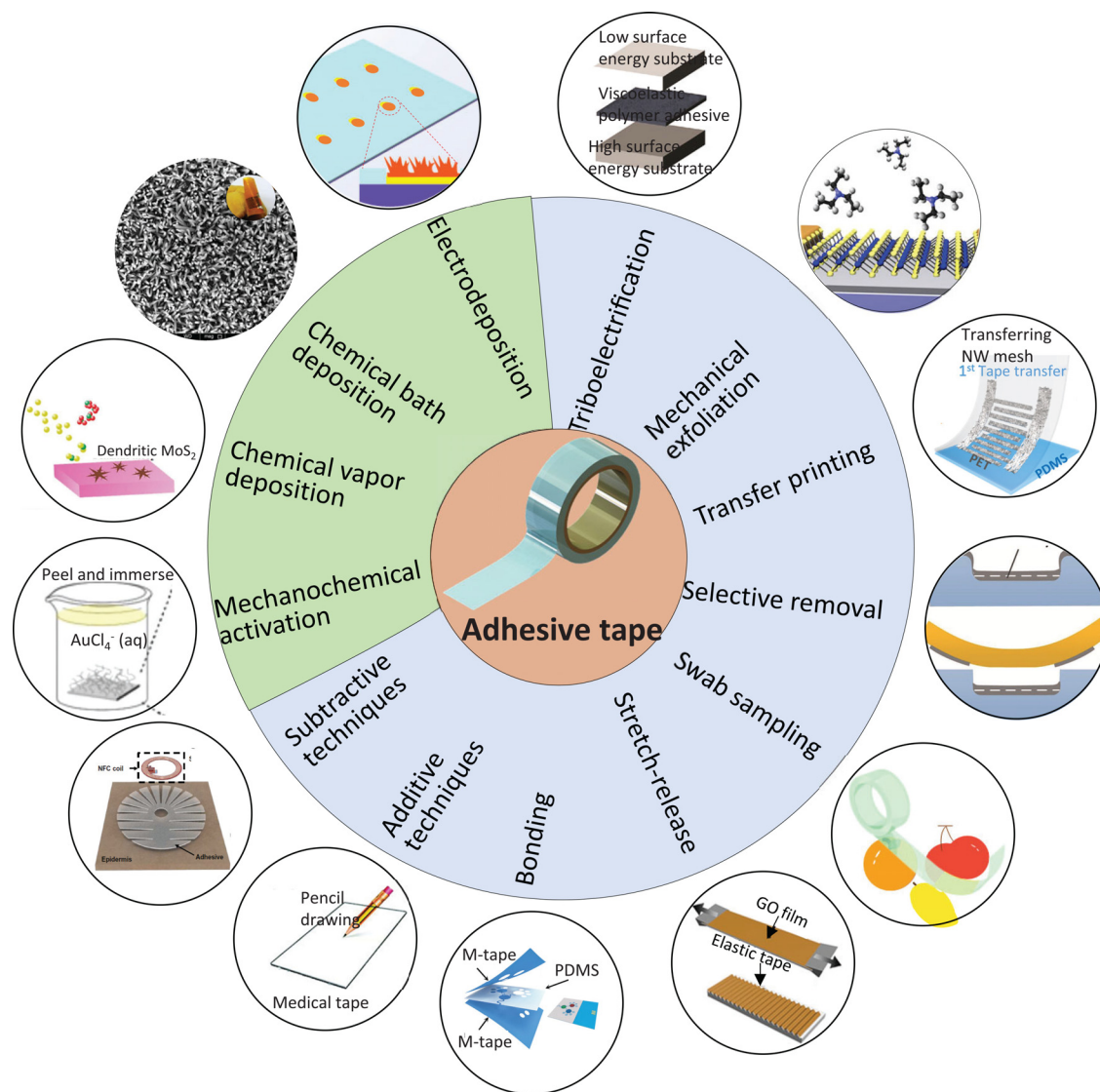
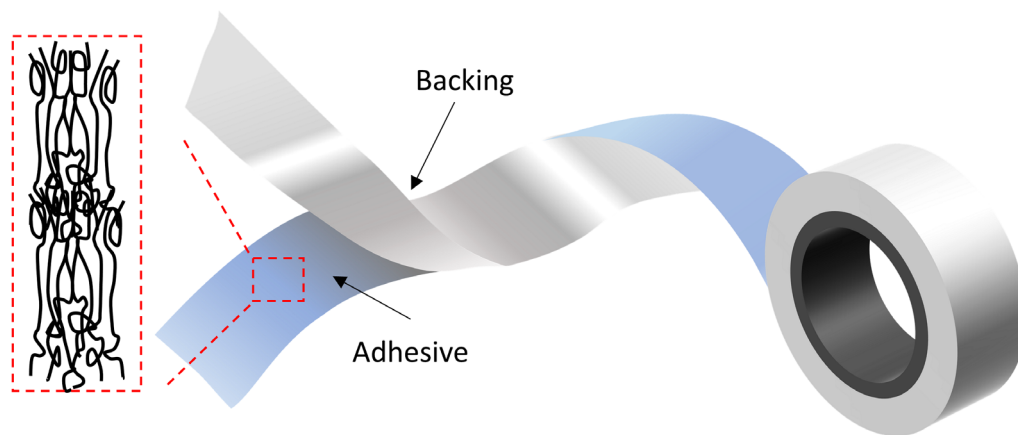


FIG. 1. Adhesive tapes-enabled material fabrication techniques and flexible electronics counterparts. Triboelectrification—surface electrification on a viscoelastic polymer adhesive surface by bonding/debonding with two substrates. Reproduced with permission from Gong *et al.*, *Adv. Mater.* **32**, 1907948 (2020). Copyright 2020 Wiley-VCH.³⁰ Mechanical exfoliation—a single monolayer of MoS₂ fabricated by the Scotch tape method for triethylamine detection. Reproduced with permission from Perkins *et al.*, *Nano Lett.* **13**, 668 (2013). Copyright 2013 American Chemical Society.³¹ Transfer printing—fabrication of flexible photodetectors based on the adhesive tape-assisted transfer printing technique. Reproduced with permission from Wang *et al.*, *ACS Appl. Mater. Interfaces* **10**, 16596 (2018). Copyright 2018 American Chemical Society.³² Selective removal—Selective removal of excessive graphene outside the polydimethylsiloxane (PDMS) channel using adhesive tape for the high-resolution graphene pattern. Reproduced with permission from Oren *et al.*, *Adv. Mater. Technol.* **2**, 1700223 (2017). Copyright 2017 Wiley-VCH.³³ Swab sampling—extraction of analytes from the targeted objects using adhesive tapes. Stretch-release—highly stretchable graphene electrode prepared by a stretch-release technique using the elastic tape. Reproduced with permission from Xu *et al.*, *Adv. Electron. Mater.* **2**, 1600022 (2016). Copyright 2016 Wiley-VCH.³⁴ Bonding—system-level packaging of self-powered wearable microfluidic sweat sensors using PDMS and medical tapes. Reproduced with permission from Yu *et al.*, *Sci. Rob.* **5**, eaaz7946 (2020). Copyright 2020 American Association for the Advancement of Science.³⁵ Additive techniques—a wearable micro-supercapacitor enabled by pencil drawing on a medical tape. Reproduced with permission from Zhu *et al.*, *Small* **15**, 1804037 (2019). Copyright 2019 Wiley-VCH.³⁶ Subtractive techniques—A laser-cut, skin-safe, adhesive tape as skin adhesive bonding layer of sweat microfluidic electronics. Reproduced with permission from Reeder *et al.*, *Sci. Adv.* **5**, eaau6356 (2019). Copyright 2019 Authors, licensed under a Creative Commons Attribution (CC BY) license.³⁷ Mechanochemical activation—mechanochemical activation-induced radicals for *in situ* reduction of metal nanoparticles (NPs) by the immersing a peeled adhesive tape in metal salt solutions. Reproduced with permission from Baytekin *et al.*, *J. Am. Chem. Soc.* **137**, 1726 (2015). Copyright 2015 American Chemical Society.²⁷ Chemical vapor deposition—chemical vapor deposition (CVD) of MoS₂ crystals on the adhesive tape-peeled SiO₂/Si substrate. Reproduced with permission from Wang *et al.*, *ACS Nano* **12**, 635 (2018). Copyright 2018 American Chemical Society.²⁰ Chemical bath deposition (CBD)—ZnO nanorods (NRs) on Kapton tape by a microwave-assisted chemical bath deposition (CBD) for UV and hydrogen sensing. Reproduced with permission from Hassan *et al.*, *Mater. Sci.-Pol.* **31**, 180 (2013). Copyright 2013 Elsevier.³⁸ Electrodeposition—electrodeposition of Au nanodendrites (NDs) on a conductive carbon tape for portable surface-enhanced Raman scattering (SERS) detection of food residues. Reproduced with permission from He *et al.*, *Biosens. Bioelectron.* **152**, 112013 (2020). Copyright 2020 Elsevier.¹⁹

a General structure



b Adhesive mechanism

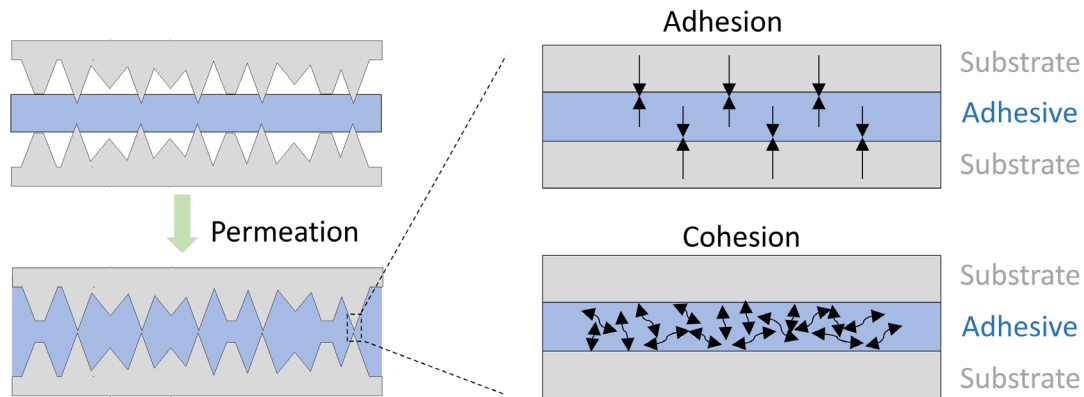


FIG. 2. General structure and adhesive mechanism of pressure-sensitive adhesive tapes. (a) The two major compositions of adhesive tapes are non-sticky backing and sticky PSA. The non-sticky backing is usually made of polymeric film, nonwoven, paper, textiles, metal foil, etc., as a physical supporting backbone. The PSA is a kind of viscoelastic polymer, producing two types of force, capable of being adhered to different adherents under slight pressure in a short period. (b) Adhesive mechanism of adhesive tapes in terms of the penetration process of PSA on the substrate and the generation of adhesion and cohesion effect. The adhesion comes from the interaction between the substrate and PSA, and the cohesion comes from the internal covalent bond, hydrogen bond, and vdWs forces from PSA itself.

of the PSA film under uniaxial extension, and k_B and T denote Boltzmann's constant and temperature, respectively.

According to this equation, there are two main prerequisites for achieving a favorable adhesive effect. First, a PSA material must possess high molecular mobility (D) with long-term relaxation processes (τ) and fluidity to penetrate the surface roughness of a substrate [Fig. 2(b), left]. In this way, close contact between the PSA and substrate can be generated [Fig. 2(b), top right].^{51,52} The interaction between the substrates and most PSAs is adhesion, which comes from vdWs force only (the vdWs force exists for all contacted systems).^{53,54} Second, a PSA material must have certain intermolecular strength and elasticity (can be equal to σ_b), which is essential to resist the debonding stress and dissipate the mechanical energy of adhesive bond failure under a peeling force.⁵² This interaction is cohesion, which comes from the covalent bond, hydrogen bond, and vdWs forces from PSA itself [Fig. 2(b), lower right]. The apparent adhesive behavior of PSA-type adhesive tape is a synergistic effect of cohesion and adhesion of the PSAs.⁵⁵

III. COMMON ADHESIVE TAPES USED IN FLEXIBLE ELECTRONICS

Various combinations of sticky adhesives and non-sticky backings contribute to different types of adhesive tapes. Figure 3 shows several representative adhesive tapes that are widely used in flexible electrical. Their typical structures, properties, and application scenarios are also briefly presented.

A. Scotch[®] tape series

Scotch[®] tape series are usually regarded as the most common commercial adhesive tape. In general, Scotch[®] tape series consist of rubber adhesive and polyester backings. However, it is worth noting that as a trademark brand of the 3M[™] Company, Scotch[®] brand tapes include many different subtypes, and each of them may have different (more or less) compositions and structures. For example, Scotch[®] Cellophane Tape [Fig. 3(a)] consists of cellophane film

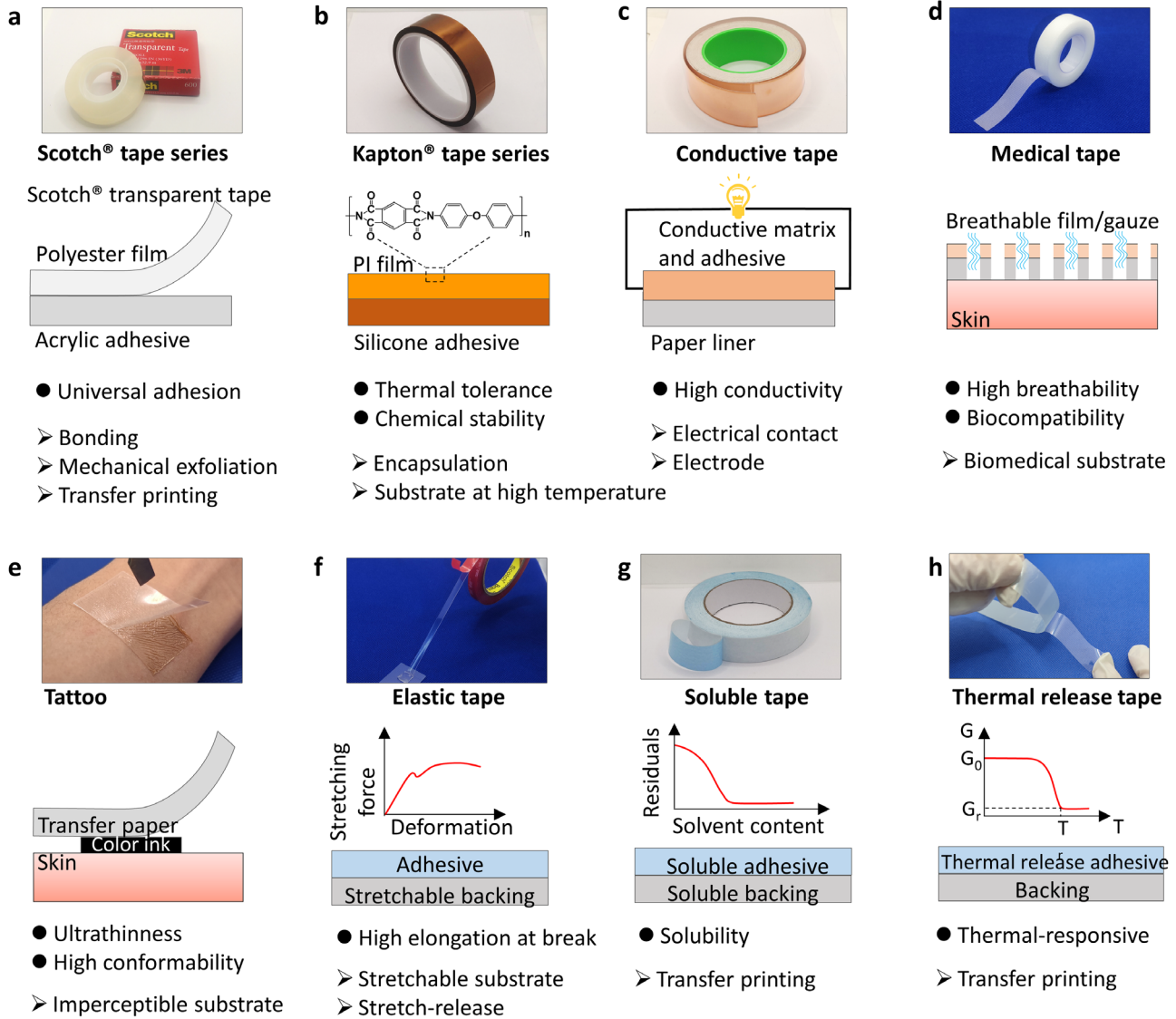


FIG. 3. Several common adhesive tapes in flexible smart electronics, including (a) Scotch® tape series, (b) Kapton® tape series, (c) conductive tape, (d) medical tape, (e) tattoo, (f) elastic tape, (g) soluble tape, and (h) thermal release tape (TRT). The respective actual photograph, structure, feature, and application scenario of each adhesive tape are briefly represented, which should be fully understood before the construction of specific flexible electronic devices. It is worth noting that some self-design adhesive materials (e.g., functional hydrogels) are not the focus of this paper. Instead, the term adhesive tapes in this review refers to off-the-shelf commodities with a clear commercial brand.

backing and acrylic PSA, which is highly transparent (also named Scotch® Transparent Tape) and can provide immediate adhesion to a variety of substrates.⁵⁶ High transparency is a desirable feature for optical or optoelectronic devices, where the light beam can be directly excited and received through the Scotch Transparent Tape.^{57,58} Scotch® Magic™ Tape is frosty on the roll, but invisible on the adhered item. Unlike glossy-finish Scotch® cellophane tape, it can be written with a pen, pencil, or marker on the matte-finish cellulose acetate backing.⁵⁹ Scotch® Double coated tape, as the name indicated, is coated with acrylic adhesive on both sides.⁶⁰ This double-sided adhesive behavior

plays a significant role in the assembly of multilayered structures of sophisticated flexible electronics.⁶¹ Due to the merits of low cost, stickiness, and flexibility, Scotch® tape series are broadly used in daily life and scientific research areas.^{62,63} One fundamental function of Scotch tape in flexible electronics is the Scotch tape test (peeling test), where the adhesion force of the electronics to the substrate is measured with a specific angle to evaluate the bonding effect between the target and substrate.^{64,65} Additionally, the term “Scotch tape method” has been given to the mechanical exfoliation of 2D vdWs materials, due to the impressive contribution of Scotch tape (will be discussed in Sec. IV A 2).

B. Kapton[®] tape series

DuPont[™] Kapton[®] tape series, also called polyimide (PI) tape, is another important type of adhesive tape. Kapton[®] tape series usually consist of brown, transparent PI films and silicone adhesive. Compared to other adhesive tapes, excellent temperature tolerance is the distinct property of Kapton[®] tape series due to the presence of PI backing [typically containing multi-plane rigid aromatic rings, Fig. 3(b)] and heatproof PSA. Kapton[®] tape series can work at a wide temperature ranging from -269 (-452 °F) to 260 °C (500 °F).^{66,67} Some other desirable performances, such as radiation resistance, electrical insulation, chemical, and mechanical stability can also be found in Kapton[®] tape series. These superior features make Kapton[®] tape series extremely favorable as a stable supporting substrate,⁶⁸ or as a protective encapsulation/packing layer of electronic elements for flexible electronics.^{13,69,70} Hassan *et al.* proposed a flexible Kapton tape-based UV and hydrogen sensor.³⁸ Briefly, a ZnO seed layer was first deposited on the Kapton tape substrate, and then ZnO nanorods (NRs) gradually grew based on the ZnO seed layer. The favorable thermal resistance of Kapton tape is necessary for ensuring stable sensing performance of UV and hydrogen at 150 °C and even 200 °C. It is obvious that most regular adhesive tapes cannot work at such a high temperature.

C. Conductive tape

Conductive tape [Fig. 3(c)] is constructed by combining the conductive matrix and PSA and supplied on a paper liner for easy handling and cutting. As the name indicates, electrical conductivity is a distinct difference in contrast to routine adhesive tapes. Conductive metallic tape and conductive carbon tape are the two main types of conductive tape. The conductive metallic tape consists of conductive metallic foil (e.g., copper, nickel, or a combination of them) as well as conductive acrylic (its exact composition is an industrial trade secret).^{71,72} Traditionally, the conductive metallic tape is employed for shielding electromagnetic interference and static charge draining.⁷³ The carbon adhesive tape (CAT) is made by filling polyester adhesive with carbon black, which is initially used to fix samples for scanning electron microscopy or energy-disperse spectroscopy analysis.

When used in flexible electronics field, these conductive adhesive tapes usually act as various conductive elements, involving electrodes, conductive pathways, etc.^{74,75} For example, copper conductive tapes possess a very low rate of electrical resistance, which can provide reliable point-to-point electrical contact for wearable sensors.^{76–78} CAT can be regarded as a flexible carbon-derivative electrode material.^{79,80} An interesting work has proved that the carbon-derived CAT can selectively adsorb NO_2 gas molecules and generate electrical conductance responsiveness.⁸¹ The NO_2 gas over the CAT-based electrode surface caused augmented electrical conductance along with the increased NO_2 gas molecules. Such a CAT-based gas sensor could distinguish NO_2 as low as 5 ppm.

D. Medical tape

Adhesive tapes have a long history of biomedical applications. In 1845, surgeons started to apply natural rubber adhesives onto a strip of cloth as surgical tape, which is usually regarded as the embryonic format of medical tape. Thereafter, Johnson & Johnson company invented the first commercial medical bandage in 1920 by integrating

gauze with PSA.⁸² Nowadays, commercial medical tape, such as the well-known Band-Aid[®], is nowadays a necessity in households and hospitals. The most distinct feature of medical tapes is their biocompatibility, which can reduce potential irritations of flexible electronics to the human body. The biocompatibility is benefitting from a biocompatible adhesive layer, which is made by medical nontoxic acrylic coating, pure natural maleic glue, medical nontoxic solvent glue, or medical nontoxic water emulsion, etc., on polymer or gauze backings. The polymer or gauze backings of medical tapes are usually porous [Fig. 3(d)]. Thus, the physiological comfort of medical tape, especially breathability, is greatly improved.⁸³

The medical tape has been widely used as a biocompatible substrate in wearable healthcare electronics, such as wound management,^{85,86} drug delivery.^{87–91} Wound biomarkers, inducing temperature, humidity, pH, oxygenation, uric acid, etc., have been monitored using medical tape-based bioelectronics.^{84,92,93} Importantly, the air permeability of medical tapes reduces the potential threat of anaerobic respiration, which is very important for wound-related bioelectronics during long-term wearing. Promoting wound healing with physical or chemical techniques based on adhesive tapes is an important issue of wound management. An interdigitated Au/Ti electrode array was fabricated onto a piece of medical tape (“band-aid”).⁹⁴ Applying low-voltage electrical stimulation was able to accelerate fibrin formation without excessive heat effect. Ogawa *et al.* presented a drug patch based on chemical iontophoresis.⁹⁵ The breathability of medical tape allowed O_2 permeability, which was conducive to the enzyme-catalytic reaction involving the oxidation of fructose, yielding a transdermal iontophoretic current ionic, guiding the small molecules (ascorbyl glucoside and rhodamine B) to penetrate the dermal barrier.

E. Tattoo

Commercially available tattoo is mainly composed of transfer paper, color ink, glue, and adhesive lamination layer.⁹⁶ Tattoos provide an epidermal temporary-transfer platform, where the color ink on the adhesive lamination layer can be transferred to the skin through pressing and peeling of the transfer paper [Fig. 3(e)]. The electronic elements with various designed patterns can be concealed in the tattoo artwork, with a protective layer made from a transparent film. After removing the transparent film, the electrode arrays are exposed and transferred onto the skin.⁴ The distinct advantages of tattoos are ultra-thinness, imperceptibility. Therefore, tattoos are widely adopted in epidermal electronics in a rather “inconspicuous” manner without any disruptions to end-users’ routines. Benefitting from the ultra-thinness, the ultra-thinness, tattoos can be easily to be conformably contacted with the curved surface of the skin. For example, when a tattoo-based wearable sweat sensor underwent bending, twisting, and stretching to check its resistance to these strains and for the presence of potential cracks or breaks in the electrode interface. Throughout the test, no apparent cracks were found and that the tattoo remained in good contact with the skin.¹⁰ Wang’s group presented many tattoo-like electrochemical sweat sensors, capable of adhering and conforming to the epidermis for biosensing of different biomarkers in sweat.^{10,96–101} In this system, conformal wireless readout circuits were fabricated on a body-compliant temporary tattoo by a screen-printing technique (will be discussed in Sec. IV A 8). The same group also introduced a tattoo-based epidermal alkaline rechargeable Ag–Zn battery to power body-worn electronic devices.¹⁶

F. Elastic tape

The stretchability of routine adhesive tapes is relatively weak. The elastic tape has a stretchable backing [Fig. 3(f)], which is made from elastic textiles, rubber, foam, or other materials with a large elongation at break, and the PSA is mainly made of acrylics. Scotch[®] Stretchable Tape series have special polypropylene film backing with elongation at breakup to $\sim 700\%$.¹⁸ 3M[™] VHB[™] is another commercial elastic tape series, which can provide high strength, high elasticity, and long-term durability.¹⁰² Elastic tape is a common substrate for stretchable electronics, and it is widely used to fabricate functionalized electronic elements by stretch-release operation (Sec. IV A 6). In this way, stretching induces stress in the materials, and crumple structures are created after releasing the stress. The synergetic effect of high stretchability and adhesive behavior ensures tight attachment between the electronic components and elastic tape during the whole stretch-release process. These crumple structures are stretchable with a high specific surface area.¹⁰³ Xu *et al.* fabricated a solid-state electrochemical capacitor with large areal-specific capacitance using elastic tape.³⁴ A layer of graphene oxide (GO) was first prepared by blade-coating GO dispersion on a prestretched elastic tape (VHB[™] acrylic 4910, 3M[™], Inc.) after thermal annealing. The GO film was then compelled into a wavy microstructure after releasing the stretched elastic tape and reduced by hydroiodic acid, yielding a stretchable reduced GO (rGO) film on the elastic tape for flexible energy devices and electronics.

G. Stimuli-responsive tape

The stimuli-responsive of tapes in this paper mainly involve soluble tapes and thermal release tapes (TRTs). Soluble tapes can be dissolved by corresponding solvents, such as water⁸ and acetone.¹⁰⁵ Taking water-soluble tape as an example, it has water-soluble backing (e.g., polyvinyl alcohol) and water-soluble PSA [Fig. 3(g)].^{106,107}

TRTs consist of thermal-responsive PSA and polyester backing. The thermal responsive PSA has a characteristic transition temperature (T_r), thus the adhesive behavior of TRT can be controlled by adjusting external temperatures. Here, a parameter of energy release rates (G) is introduced to better describe this process. The parameter G represents the energy of interfacial bond breaking and adhesive dissipation around the crack tip according to Griffith criterion,¹⁰⁸ which can be given according to the following equation:¹⁰⁹

$$G_{TRT/object}(T) \begin{cases} -e^{\gamma(T-T_r)+\ln(G_0-G_r)}, & T \leq T_r, \\ G_r, & T > T_r, \end{cases}$$

where e indicates the Euler's constant, T denotes the current temperature, and G_0 and G_r are the initial critical energy release rate and the critical energy release rate when the adhesive behavior on TRT is deactivated, respectively. γ is a parameter related to the compositions of materials. The curves are roughly plotted in Fig. 3(h). The adhesion strength of TRT is strong at low temperature ($<T_r$) settings, however, it significantly weakens when the temperature is above T_r , making TRT readily removable from the bonded surface.¹⁰⁹ Overall, these two stimuli-responsive tapes can serve as an intermediary sacrificial material for the temporary transfer and bonding of targeted electronic elements, and selectively removing them away from the whole system is allowed by applying external stimulus.¹⁰⁴

IV. ADHESIVE TAPE-ASSISTED MATERIALS AND DEVICES

The prerequisite of flexible smart electronics is the rational design and configuration of electronic elements. In this review, adhesive tapes dominate these design and configuration processes, which can be categorized into physical and chemical modifications, depending on the specific operating mechanisms. With these adhesive tape-enabled physical and chemical techniques, a variety of up-to-date electrodes, circuits, and connecting competent, device skeletons can be achieved for diverse flexible electronics (Table 1). In this section, we will describe each physical or chemical modification technique and the flexible device counterpart in detail, with a focus on how the properties (e.g., stickiness, flexibility, conductivity) of various adhesive tapes set the stage for the related techniques and devices.

A. Physically-dominated techniques

1. Triboelectrification

Peeling off adhesive tapes seems a simple operation in daily life; however, it is actually a complex process at the microscale level involving polymer chain rearrangement, orientation, as well as slippage.¹²³ Pulling off PSAs from the backings at routine speeds (cm/s) associates homolytic and heterolytic cleavage along the separation/displacement direction,^{124,125} which can result in surface radicals and charged species [Fig. 4(a), left]. Some characterization techniques have been developed to visualize these surface radicals and charged species. Surface radicals can be observed by magnetic force microscopy [MFM, Fig. 4(a), middle]. These surface radicals can induce chemical reactions, which will be emphasized in Sec. IV B 1. The charged species possess a net/macroscopic charge on the order of few nC/cm², which can be characterized by a homemade Faraday cage linked to an electrometer.²⁷ Kelvin force microscopy (KFM) mapping further indicates that the "mosaics"-like surface potentials are nonuniformly distributed [Fig. 4(a), right]. In this section, we focus on these charge species, which can produce triboelectrification at the adhesive-substrate interface. The relevant phenomenon, mechanism, devices, and applications will be discussed in detail.

Numerous researchers have found that peeling off adhesive tapes from the intrinsic backings leads to an electric field and yields electromagnetic radiation at radiowave,¹²⁶ terahertz,¹²⁷ visible,^{128,129} and x-ray level.¹³⁰⁻¹³² Sometimes, these electromagnetic radiations with photon generation are also called triboluminescence.¹³³ In this process, PSA and backing are positively and negatively charged, respectively. X-ray is extremely amazing because the energy required for x-ray photons is usually about 4–5 orders of magnitude higher than that provided by the vdWs interaction between adhesive and backing.^{128,134} The explanation can be sought in the energy density focusing mechanism.¹³⁵ Peeling off the adhesive tape in a moderate vacuum enables simultaneous emission of visible and x-ray.¹⁴ As shown in Fig. 4(b), the blue light and red patch near the peel point arose from the scintillator responsive to x-ray energies and the neon-improved visible light in a vacuum environment. X-ray imaging of a human finger was also available using this facile strategy. The generated x-ray pulse was correlated with radio frequency pulses and slips in the force during peeling off the adhesive tapes. Other parameters, such as the gas pressure, peel speed, type of adhesive tape, and detector angle, also have a significant impact on x-ray radiation during peeling off adhesive tapes.^{129,130,132} To some extent, the peeling point can be simplified as a

TABLE I. Emerging flexible electronics enabled by adhesive tapes. Note: PEDOT:PSS: poly(3,4-ethylenedioxythiophene)/polystyrenesulfonate, PEN: polyethylene naphthalene, CNT: carbon nanotube, FEP: fluorinated ethylene propylene, ITO: indium tin oxide.

Roles of tape	Tape types	Electronic components	Applications	Refs.
Tape-peeling charging	Lyreco, polypropylene substrate with acrylic adhesive	FEP electret film	Triboelectrification devices	110
Mechanical exfoliation	Scotch tape	Monolayer MoS ₂	Gas sensors	31
Mechanical exfoliation	Scotch tape	Multilayer black phosphorus	Gas sensors	111
Mechanical exfoliation and supporting substrate	Scotch tape	MnO ₂ nano-grass electrode	Supercapacitor	112
Transfer printing	Water-soluble tape	TiO ₂ nanomembrane /Au Nanoparticles	Drug delivery	8
Electrode	Conductive copper tape	PEDOT:PSS	Gas sensors	113
Swab sampling	Unknown transparent tape	Au nanoparticles	SERS sensors	114
Swab sampling	Unknown transparent tape	Al ₂ O ₃ -coated Ag nanorods	SERS sensors	57
Stretch-release	Elastic tape	Scale-like graphene	Wearable strain sensors	6
Stretch-release and supporting substrate	Elastic Tapes	Wavy GO films	Supercapacitor	34
Selective removal	Kapton tape	Silver NWs	Wearable strain sensors	115
Conformal substrate	Medical tape	Au/PEN electrode with hair structure	Wearable pressure sensors	116
Encapsulation and epidermal adhesive layer	Medical tape	Au and Ag/AgCl electrode	Sweat sensors	117
Supporting substrate	Tattoo	Ag and Zn electrode	Battery	16
Lamination and encapsulation layer	Cu conductive tape	Perovskite	Battery	118
Supporting substrate and epidermal adhesive layer	Medical tape	MnO ₂ /graphite	Supercapacitor	36
Bonding layer	Kapton tape	ITO	Triboelectrification devices	13
Supporting substrate and epidermal adhesive layer	Kapton tape and medical tape	Carbon electrode	Wound management	92
Supporting substrate and epidermal adhesive layer	Medical tape	Au electrode	Wound management	94
Encapsulation of drug	Kapton tape	Ag electrode	Drug delivery	119
Encapsulation of drug and epidermal adhesive layer	Medical tape	Enzyme-modified carbon fabrics, ascorbyl glucoside (drug)	Drug delivery	95
Supporting substrate	Scotch tape	Ag nanoparticles on SiO ₂ NWs	SERS sensors	120
Template	Medical tape	Ag@CNT	Wearable pressure sensors	121
Microfluidic layer	Medical tape	Carbon and Ag/AgCl electrodes	Sweat sensors	61
Conductive pathway	Ni-coated textile tape	Carbonized silk electrode	Sweat sensors	122
Electrode	CAT	PDMS negative tribo-layer, Ni foil as the electrode for the PA6 positive tribo-layer.	Triboelectrification devices	80
Electrode	CAT	Intrinsic carbon on CAT	Gas sensors	74

parallel plate capacitor [Fig. 4(c)]. Thus, the electrostatic force F_E can be evaluated from

$$F_E = \frac{\gamma_p}{\gamma_{tot}} F_A,$$

where γ_p and γ_{tot} are the polar part of the surface energy and the total surface energy, respectively. F_A is the apparent adhesive force of adhesive tape. Thus, the output voltage U can be given¹³¹

$$U = \sqrt{\frac{\gamma_p F_A d^2}{\gamma_{tot} \epsilon_0 \epsilon_r A}},$$

where the parameters include dielectric constant ϵ_0 , the sample permittivity ϵ_r , plate distance d , and plate facing area A . Although regarding the peeling point as a plate capacitor is a crude assumption that needs to be further deliberated, the equation releases approximate guidance about how to maximize electron acceleration voltage, such as

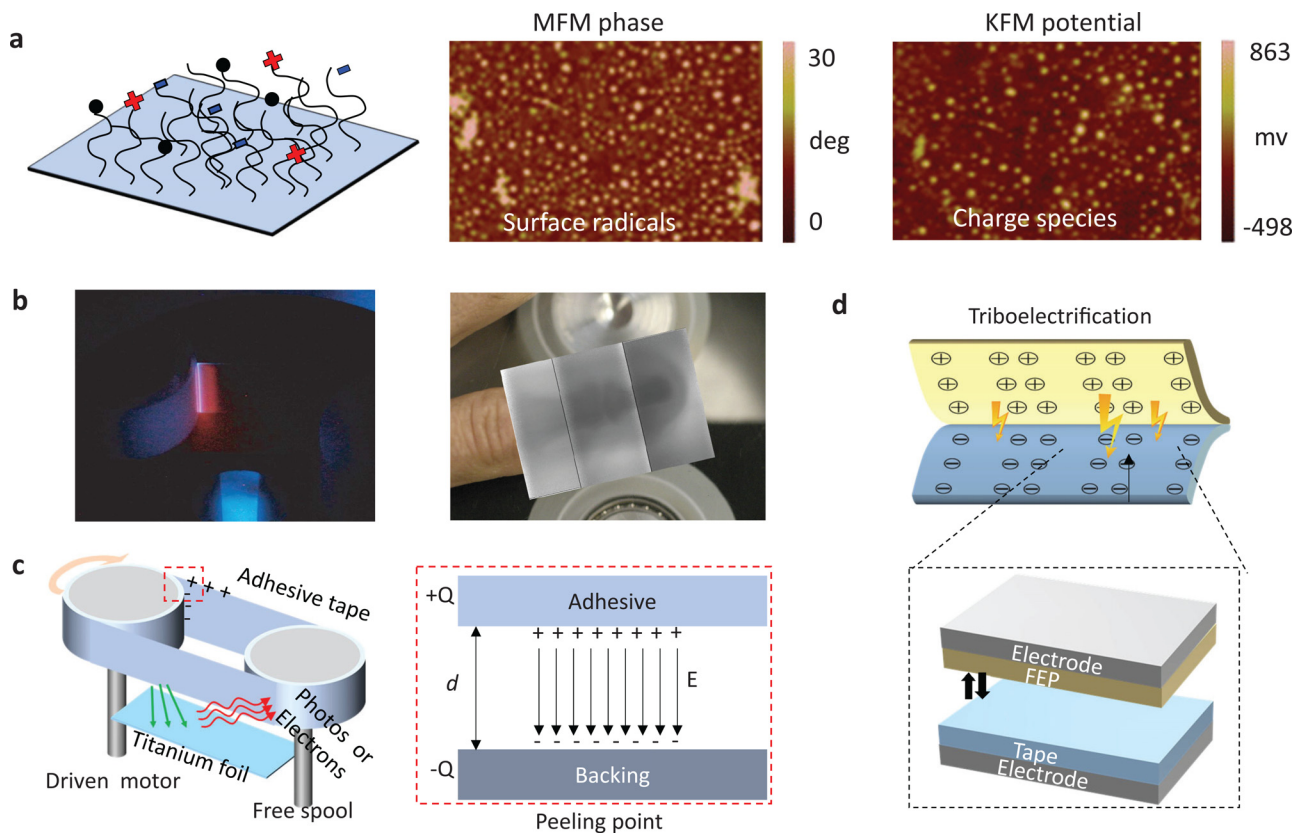


FIG. 4. Triboelectrification. (a) Mechanoradicals and charged species generated during pulling off adhesive tapes. Magnetic force microscopy (MFM) map of mechanoradicals (white spots), and Kelvin force microscopy (KFM) map of the charge mosaics with both positive and negative regions. MFM and KFM are reproduced with permission from Baytekin *et al.*, *J. Am. Chem. Soc.* **137**, 1726 (2015). Copyright 2015 American Chemical Society.²⁷ (b) Simultaneous emission of visible and x-ray photons during peeling off the tape (left) and the corresponding x-ray imaging of a human finger (right). Reproduced with permission from Camara *et al.*, *Nature* **455**, 1089 (2008). Copyright 2008 Nature Publishing Group.¹⁴ (c) Schematic of electromagnetic radiation during peeling off adhesive tapes and the simplified plate capacitor model at the peeling point. Reproduced with permission from Stocker *et al.*, *J. Electrostat.* **71**, 905 (2013). Copyright 2013 Elsevier.¹³¹ (d) A triboelectric nanogenerator (TENG) by peeling a fluorinated ethylene propylene (FEP) film away from adhesive tape. Reproduced with permission from Zhang *et al.*, *Nano Energy* **48**, 256 (2018). Copyright 2018 Elsevier.¹¹⁰

choosing adhesive tapes with relatively high adhesive force F_A and creating a high ratio of γ_p/γ_{tot} .

The triboelectric nanogenerator (TENG) is well known as a miniaturized, facile, low-cost energy harvesting device that converts ambient energies (e.g., body motion, acoustic waves, heat, winds, and water flow) into electricity. The mechanism of TENG is the coupling effects between triboelectrification and electrostatic induction through contact separation (contact electrification) or relative sliding between two materials with opposite triboelectricity.¹³⁶ Electrification phenomenon induced by the peeling PSAs of adhesive tapes from the bonded surface (including the intrinsic backing and other substrates) is quite like the TENG based on the contact-separation mechanism.^{137,138} To verify this perspective, a viscoelastic polymer adhesive was bonded with two substrates of high and low surface energy, then debonded away from the low surface energy substrate and maintained on the high surface energy.³⁰ This process caused the breaking of polymer chains at an atomistic level, producing macroscopic surface electrification. Based on this strategy, such a device ($0.5 \times 0.5 \text{ cm}^2$) achieved an average output power density of $216.7 \mu\text{W cm}^{-2}$, which was about 1.5

times that without a viscoelastic polymer adhesive layer. Similarly, Zhang *et al.* designed a TENG device based on a facile tape-peeling charging method.¹¹⁰ A piece of adhesive tape was attached to a fluorinated ethylene propylene (FEP) electret film followed by peeling off. As a result, the sticky acrylic adhesive on the tape was positively charged, and the FEP film was negatively charged, respectively, generating an electric field between the two polymer films [Fig. 4(d)]. The resulting electric field was attributed to the wide gap between acrylic and FEP in the triboelectric series.

2. Mechanical exfoliation

Mechanical exfoliation also called the “Scotch tape method,” is a famous technique for the fabrication of 2D vdWs layered materials with a long history back to the 1970s.¹³⁹ The Scotch tape method makes mechanical exfoliation extremely easy even at home: a piece of Scotch tape is applied to the bulk 2DMs surface and then just peeled off. This process is repeated until thin few/single-layer 2DM are obtained [Fig. 5(a), left and middle]. During this process, the vdWs

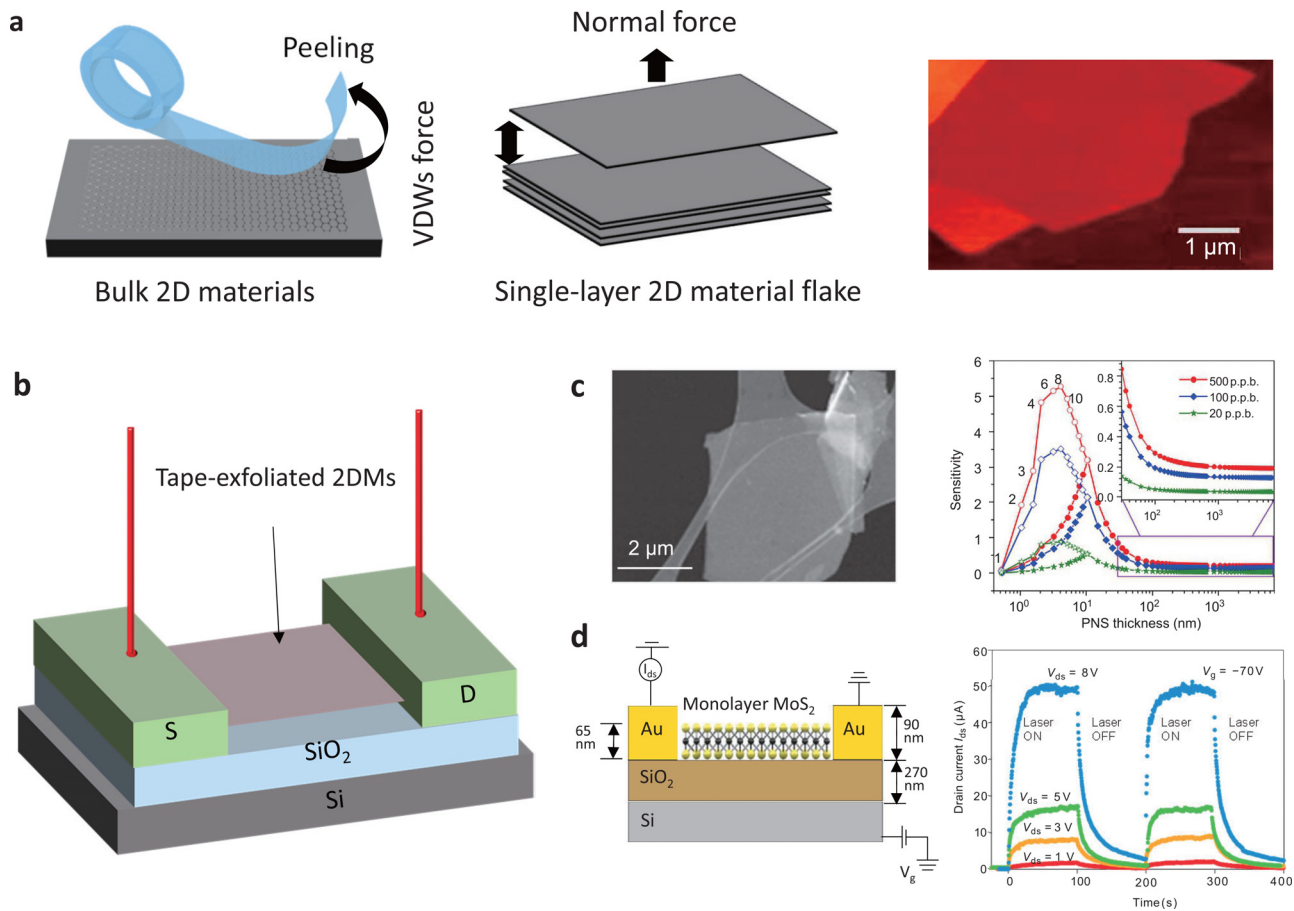


FIG. 5. Mechanical exfoliation. (a) Mechanical exfoliation of single-layer 2DMs from bulk graphite based on the famous Scotch tape method, during which the vdWs attraction among adjacent 2DMs flakes is overcome by the micromechanical cleavage (left and middle). An atomic force microscopic (AFM) image of single layer graphene (right), Reproduced with permission from Novoselov *et al.*, *Science* **306**, 666 (2004). Copyright 2004 American Association for the Advancement of Science.²⁵ (b) Schematic of monolayer 2DMs fabricated by the Scotch tape method for transistor research. (c) Mechanically exfoliated phosphorene nanosheet (PNS) for detection of NO_2 . Reproduced with permission from Cui *et al.*, *Nat. Commun.* **6**, 8632 (2015). Copyright 2015 Authors, licensed under a Creative Commons Attribution (CC BY) license.¹⁴⁷ (d) Ultrasensitive photodetectors enabled by monolayer MoS_2 using the Scotch tape method. Reproduced with permission from Lopez-Sanchez *et al.*, *Nat. Nanotechnol.* **8**, 497 (2013). Copyright 2013 Nature Publishing Group.

attraction among adjacent 2DMs flakes is overcome by the micromechanical cleavage upon peeling adhesive tapes away from the target 2DMs surface.^{140,141} The most famous case is that two physicists exfoliated a single layer of graphene [most distributed in the central brown-red area in Fig. 5(a), right] from the bulk graphite using the Scotch tape in 2004,^{25,142} and they won the Nobel Prize in Physics in 2010. Following this revolutionary discovery, a wide variety of single/few-layer 2DMs have been intensively investigated, including MoS_2 , WSe_2 , black phosphorus, and topological insulators (e.g., Bi_2Te_3 , Bi_2Se_3 , Sb_2Te_3).^{142–145} Up to now, mechanical exfoliation is a dominant technique for the fabrication of various layers of 2DMs in a laboratory without any other auxiliary materials, reagents, or tools. However, the traditional Scotch tape method is limited by low yields and small lateral sizes, which is incompatible with industrial-scale manufacturing. Recent work has achieved a monolayer of 2D vdWs crystals with macroscopic dimensions (from millimeters to centimeters) in a high-throughput manner based on a modified mechanical

exfoliation method.¹⁴⁶ Briefly, a gold film was deposited on a highly polished (atomically flat) silicon wafer, followed by spin-coated a polyvinylpyrrolidone (PVP) interfacial layer. The gold and PVP layer were then transferred to a TRT, and the resulting TRT was applied on the bulk vdW crystal. The ultraflat gold layer on TRT allowed uniform and intimate contact with 2D vdW crystal. Then, the scientists can exfoliate a single-crystal monolayer with macroscopic dimensions after removing TRT, PVP, and gold.

These single/few-layer 2DMs using the Scotch tape have many outstanding properties such as ultimate size scaling and ultrahigh surface area-to-volume ratio compared to their bulk counterparts. In particular, the 2D semiconductor materials enabled by the Scotch tape method have contributed to a surge in field-effect transistors (FETs) study,¹⁴⁸ where the exfoliated 2DMs are usually deposited on thermal SiO_2/Si wafers and connected with two metallic electrodes (e.g., Au) pad [Fig. 5(b)].^{31,149} One important application of these FETs is gas sensors. These 2DMs include graphene, semiconducting transition

metal dichalcogenides (MoS_2 , WS_2 , MoSe_2 , etc.), and layered metal oxides (MoO_3 , SnO_2 , phosphorene, h-BN, etc.).¹⁵⁰ Jonker's group has successfully detected various gases including trimethylamine [a nerve gas by-product, Fig. 5(c)], acetone, and trimethylamine with high sensitivity and selectivity.^{31,151} Further studies indicate that the thickness of 2DMs has a significant influence on analytical sensitivity. For a phosphorene nanosheet (PNS)-based FET gas sensor, the relationship between sensitivity and PNS thickness can be roughly expressed as¹⁴⁷

$$S(t) \propto \frac{\Delta Q}{t} \exp\left(\frac{E_g - 2|E_F - E_{Fi}|}{2K_B T}\right),$$

where ΔQ , t , and $|E_F - E_{Fi}|$, K_B and T denote the total charge transfer from the PNS to the gas molecules, the PNS thickness, the energy spacing between the Fermi level and the intrinsic Fermi level, and the Boltzmann constant temperature, respectively. E_g indicates the energy gap, which is dependent on the PNS thickness. The Scotch tape method provides a facile method to flexibly change the thickness by increasing or decreasing the times of mechanical exfoliation, and the theoretical (dots) and experimental (line) results are shown in Fig. 5(c) (right) with good agreement.

Another important application of these 2DMs-based FETs is photodetectors. Kis's group has demonstrated an ultrasensitive monolayer MoS_2 phototransistor using the Scotch tape method as shown in Fig. 5(d).¹⁵² Impressively, the phototransistor can be turned off, as monolayer MoS_2 is a direct-bandgap semiconductor with a bandgap

of 1.8 eV due to quantum-mechanical confinement. This contributed to low dark currents and noise equivalent power lower ($1.8 \times 10^{-15} \text{ W Hz}^{-1/2}$ for $V_{\text{drain-source}}$) than in commercial silicon avalanche photodiodes ($3 \times 10^{-14} \text{ W Hz}^{-1/2}$).¹⁵³ The device also illustrated a maximum external photoresponsivity of 880 AW^{-2} ($\lambda = 561 \text{ nm}$) and a broad spectral range of 400–680 nm range. Similar photodetectors based on single or few-layer 2DMs have been widely investigated using the Scotch tape method.^{154–156}

3. Transfer printing

Transfer printing is an indirect material fabrication process, where pre-prepared materials are peeled off from a donor substrate and transferred onto a receiver substrate using adhesive materials,¹⁵⁷ such as adhesive tapes [Fig. 6(a)].^{158–161} The adhesive force (or surface energy) differences between various interfaces are the prerequisite for successful transfer printing: the adhesive force between target materials and adhesive tapes should be stronger than that between target materials and donor substrates, while weaker than that between target materials and receiver substrate. According to the transfer times, transfer printing can be categorized into three types: single transfer printing (STP), double transfer printing (DTP), and multiple transfer printing (MTP).²⁶ As the name indicated, STP describes a single transfer printing step.^{162,163} DTP and MTP refer to two-time and multiplex transfer printing processes, which utilize the remaining adhesive force on the adhesive tape after STP.²⁶

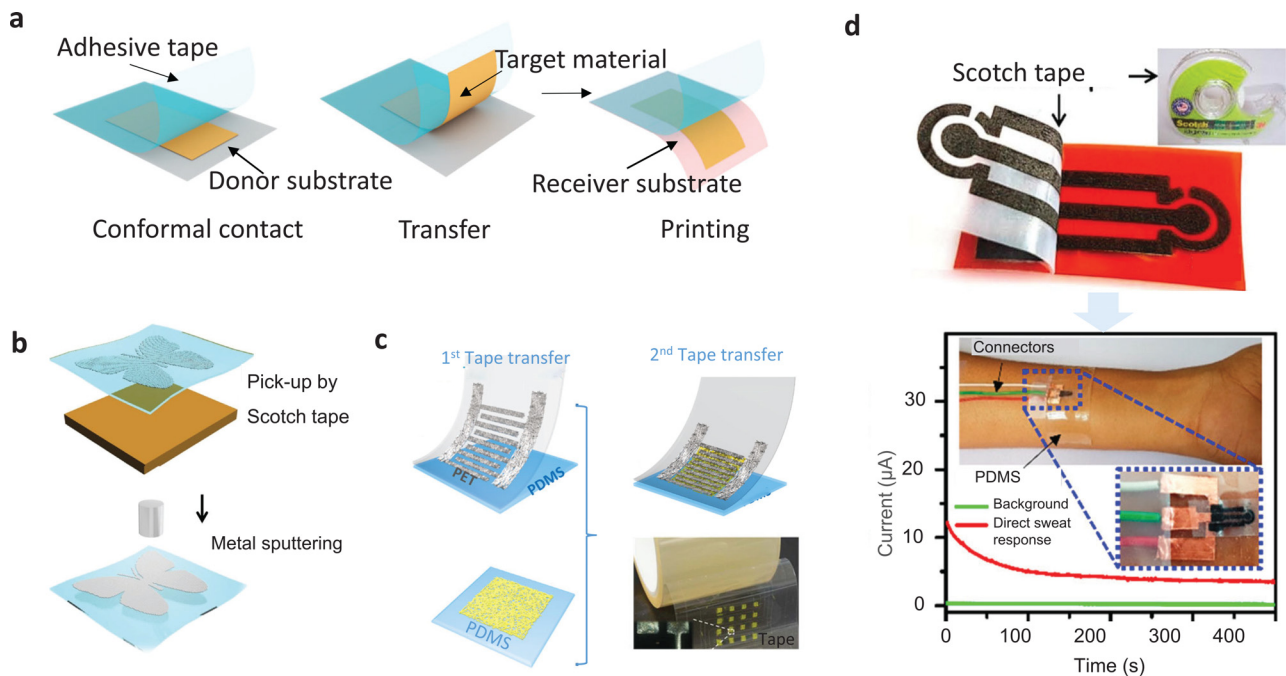


FIG. 6. Transfer printing. (a) Schematic process of transfer printing using adhesive tapes, where the target materials can be successively picked up from a donor substrate and transferred to a receiver substrate. (b) Adhesive tape-assisted single transfer printing (STP) of patterned butterfly-like plasmonic metafilm for flexible surface-enhanced Raman scattering (SERS) sensors. Reproduced with permission from Liu *et al.*, *Adv. Funct. Mater.* **26**, 5515 (2016). Copyright 2016 Wiley-VCH.¹⁶⁵ (c) Fabrication of a tape-based CdS NW photodetector using double transfer printing (DTP) technique. Reproduced with permission from Wang *et al.*, *ACS Appl. Mater. Interfaces* **10**, 16596 (2018). Copyright 2018 American Chemical Society.³² (d) Transfer printing of laser-scribed graphene (LSG) onto Scotch tape as sweat-sensing electrode arrays. Reproduced with permission from Prabhakaran and Nayak, *ACS Appl. Nano Mater.* **3**, 391 (2020). Copyright 2020 American Chemical Society.¹⁷⁰

Based on adhesive tape-assisted STP, DTP, and MTP, a wide range of nanomaterials have been developed, such as nanowires,^{32,164} films,¹⁶⁵ micro-nanoarrays.^{166,167} Transfer printing is widely used to fabricate adhesive tape-based flexible (opto)electronics, where adhesive tapes serve as the supporting substrate.^{168,169} Liu *et al.* constructed a flexible patterned plasmonic metasurface using the STP technique [Fig. 6(b)].¹⁶⁵ Briefly, monolayer polystyrene (PS) beads were closely packed on a glass or silica wafer (donor substrate) and then engraved into a butterfly pattern. Next, the resulting PS patterns were transferred onto Scotch tape (receiver substrate). Flexible plasmonic tape for SERS analysis was finally obtained by further sputtering silver film onto the PS template. Wang *et al.* proposed a tape-based photodetector using the DTP technique.³² The AgNWs interdigitated electrode was patterned and transferred onto a piece of adhesive tape. CdS NWs film was fabricated on an anode aluminum oxide (AAO) membrane and transferred onto PDMS film. Then, the CdS NWs could be further transferred from PDMS to the AgNWs-attached adhesive tape as shown in Fig. 6(c). Figure 6(d) demonstrates a miniaturized tape-based sweat biosensor for enzyme-free analysis of sweat glucose, wherein the Scotch tape allowed the complete transfer of laser-scribed graphene electrode patterns without losing electrochemical performance.¹⁷⁰ Zang *et al.* designed a composite film electrode consisting of vertically aligned CNTs coated with pseudocapacitive TiS₂ and transferred it onto Kapton tape. The resulting pseudocapacitors achieved a fine energy density of 195 F g⁻¹ in a Li-rich electrolyte.¹⁷¹

Sometimes, adhesive tapes are used as a temporary tool for transfer printing.⁴⁵ In this case, eliminating the adhesive behavior of the adhesive tape to release the target materials is a critical issue. Fortunately, the soluble tapes^{104,105} and TRTs^{109,146,172} mentioned in Sec. III G allow the on-demand release of the target electronics via controlling the temperature or applying corresponding solvents. These stimuli-responsive adhesive tapes are extremely favorable for transfer printing and releasing ultrathin target materials (e.g., monolayer graphene¹⁷³ and MoS₂¹⁷⁴) by applying the corresponding stimuli. By comparison, releasing the ultrathin target materials from routine adhesive tapes is difficult and will probably damage the ultrathin target materials. In an early work, a layer of graphene films was first grown on metal (Ni or Cu)/SiO₂ layers. A TRT (Nitto Denko Co.) was adhered to the graphene and then soaked in water.¹⁷⁵ After that, the tape/graphene/metal could be separated from the SiO₂ layer. Then FeCl₃ solution was used to further remove the metal layers, and finally, the obtained graphene on the TRT can be on-demand and completely transferred onto arbitrary substrates. The resulting graphene films can be used to fabricate FET and stretchable strain sensors. Scientists can flexibly choose the types of adhesive tapes and times of transfer printing depending on the actual requirements.

4. Selective removal

Selective removal by adhesive tape is used to create surface electronics arrays as demonstrated in Fig. 7(a). Briefly, the target materials are first applied onto a substrate, and then the non-wanted part is selectively removed using adhesive tape.¹⁷⁶ The process of selective removal is somewhat like transfer printing. The difference is that the target materials are retained on the initial substrate in the selective removal process. However, in the transfer

printing process, they are transferred away from the initial substrate and applied to other interfaces.

A master template is conducive to improving the efficiency of selective removal and the resulting microarray resolution.¹⁷⁹ Briefly, target materials are first applied to a positive or negative mold. Then, an adhesive tape is applied to generate a tight connection with the material surface. The unwanted portions of target materials on positive sites are selectively removed; conversely, target portions on negative sites are reserved. Based on template-assisted selective removal techniques, Au electrodes with sub-nanometer resolution can be achieved.¹⁷⁸ Careful attention should be taken to avoid the occurrence of damage to the target materials during the selective removal operation (e.g., due to excessive peeling force). Figure 7(b) demonstrates the fabrication of vertically oriented gaps in opaque metal films with nanoscale gap widths using an adhesive tape-assisted selective removal technique.¹⁷⁷ The Si substrate was first patterned with a metallic layer based on standard patterning techniques (e.g., optical lithography, e-beam lithography) and then deposited with a thin layer of insulator Al₂O₃ via atomic layer deposition (ALD) technique. Then the resulting hybrid layer was subsequently filled with metal by directional evaporation. The excessive second metal layer that sat on the top of the first layer was selectively removed by a piece of Scotch tape so that vertically oriented gaps in opaque metal films were created with gap widths as narrow as 9.9 Å. The resulting nanogap created by tape-assisted selective removal could uniformly extend along a millimeter-scale loop, which can be used to exploit strong THz resonances. Cui *et al.* proposed a similar strategy for the mass production of nanogap electrode arrays by integrating ALD, adhesive tape-assisted selective removal, and chemical etching, which can be used in nonvolatile resistive switches [Fig. 7(c)].

Selective removal can be combined with other tape-assisted techniques to construct flexible electronic arrays. Oren *et al.* first fabricated a thick graphene film by applying graphene suspensions onto the PDMS mold with positive and negative channels.³³ Then, a piece of Scotch tape was attached onto the positive surface of PDMS. Peeling off the adhesive tape resulted in a well-defined graphene pattern in the concave channel of PDMS, and the invented graphene partition on the top surface was selectively removed. Deeper research suggested that when the graphene film was thinner than 1.5 μm, the Scotch tape could perfectly remove the graphene film outside the channel without destroying the graphene film on the negative channels, as long as the tape was not in direct touch with it. Finally, the graphene patterns inside of the negative channel at the PDMS surface were transferred onto another Scotch tape using the transfer printing technique, achieving high-resolution graphene microarrays (20 μm in channel width) for pressure/strain sensors. Selective removal using adhesive tape can also on-demand design of the electrode materials with various shapes and sizes. For example, to fabricate the sensing material of the strain sensor, fragmented graphene foam/isopropyl alcohol solution was drop-cast onto a glass slide [Fig. 7(d)].¹⁷⁶ The dried sample was then patterned into a regular, controlled, and rectangular shape with PI tape by the selective removal of the nonpatterned part. The patterned graphene foam was transferred onto PDMS, capable of detection of bio-signals such as a pulse of the radial artery and elbow/finger bending. Control electrode shape using this selective removal strategy is so facile that can be performed without the need for skilled operators, particularly economic for resource-limited areas.¹¹⁵

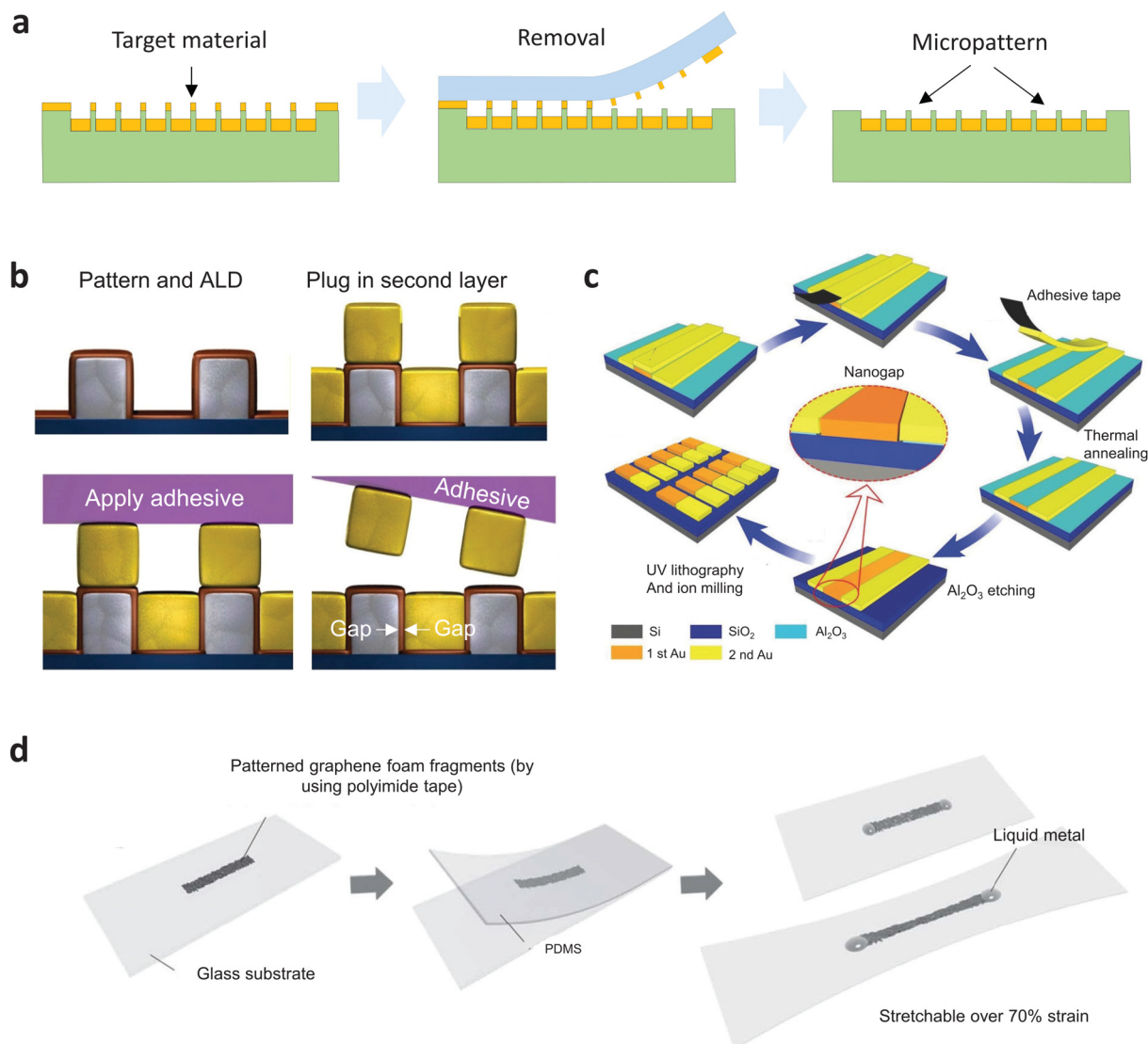


FIG. 7. Selective removal. (a) Schematic of high-resolution arrays based on selective removal technique using adhesive tapes, where target materials are first applied into a template possessing positive and negative features. Then, the unwanted portion of target materials on positive sites are selectively removed by adhesive tapes and target portions on negative sites are reserved. (b) Fabrication of vertically oriented gaps in opaque metal films with nanoscale gap widths using the adhesive tape-assisted selective removal technique. Reproduced with permission from Chen *et al.*, *Nat. Commun.* **4**, 2361 (2013). Copyright 2013 Authors, licensed under a Creative Commons Attribution (CC BY) license.¹⁷⁷ (c) Fabrication of nanogap electrode arrays for resistive random access memory, where the excessive Au layer can be selectively removed using adhesive tapes. Reproduced with permission from Cui *et al.*, *Adv. Mater.* **28**, 8227 (2016). Copyright 2016 Wiley-VCH.¹⁷⁸ (d) Modulation of the shape and size of graphene foam using Kapton tapes for high-sensitive strain sensors. Reproduced with permission from Jeong *et al.*, *Adv. Funct. Mater.* **25**, 4228 (2015). Copyright 2015 Wiley-VCH.¹⁷⁶

5. Swab sampling

Effective and rapid collection of target molecules (e.g., low-density-distribution powder, dust, and residues) from curved and complex surfaces is highly desirable for POCT applications. Adhesive tape-based sampling strategies are widely adopted in environmental, food microbiology, and healthcare, which can be traced back to the early 1950s.^{180,181} Compared to traditional rigid (e.g., glass, slide, and silicon wafers) and non-sticky flexible substrates (e.g., paper, cotton, and polymer film), adhesive tape enables rapid and convenient swab

sampling of specimens thanks to its distinct sticky feature [Fig. 8(a)]. These swab sampling techniques enabled by adhesive tapes can greatly accelerate the analytical efficiency and provide early-warning feedback.

Generally, there are two common adhesive tape-assisted sampling strategies. The first strategy is using bare adhesive tape just for collecting samples, and the sensing elements are independently constructed on other substrates [Fig. 8(b)]. In this strategy, adhesive tapes can be repeatedly used in a “paste, peel off, and paste again” manner until enough samples are collected.⁵⁷ The collected samples on the

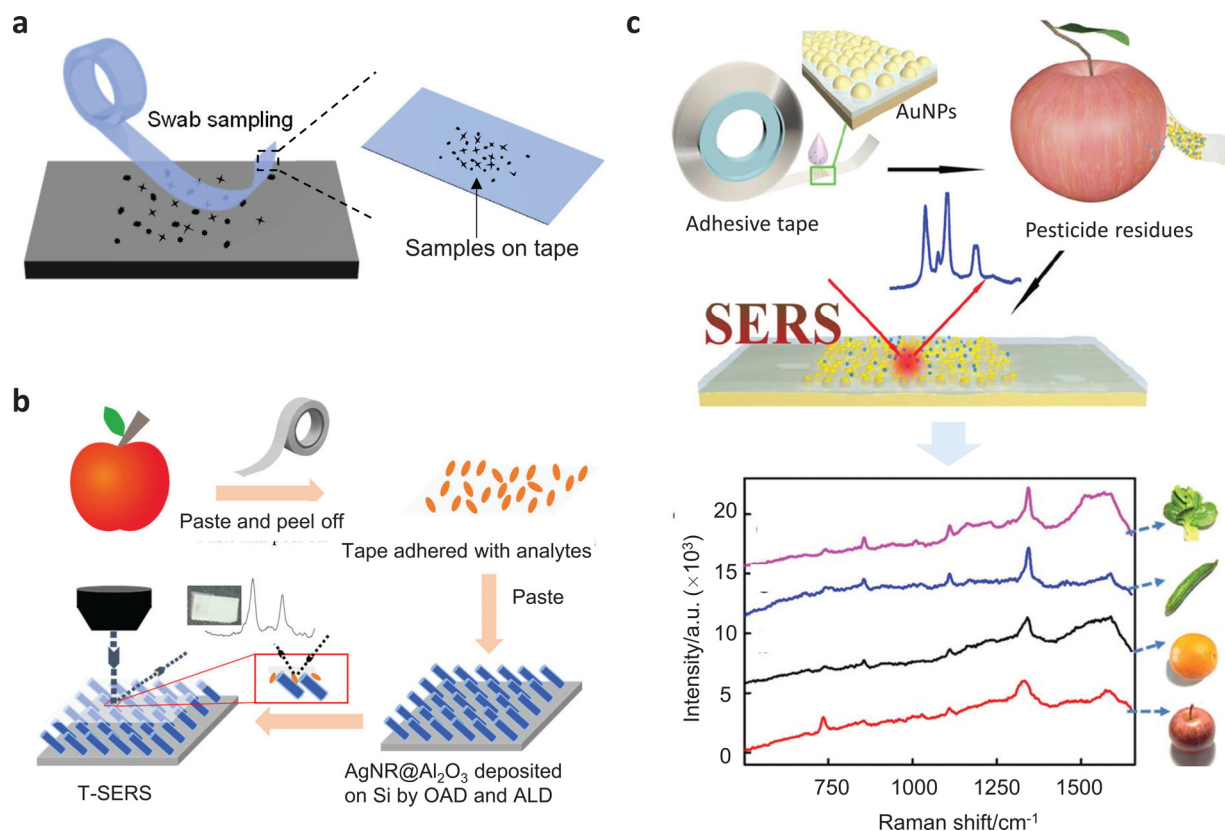


FIG. 8. Swab Sampling. (a) Schematic of swab sampling of targeted analytes using adhesive tape, where rapid and convenient sample collection on the adhesive tapes is allowed thanks to the distinct sticky feature. (b) Adhesive tape-assisted “pasting and peeling off” for collecting residues and transferring the collected residues onto the SERS substrate for SERS analysis. In this strategy, bare adhesive tape is used just for collecting sample, and SERS materials are independently constructed on other substrates. Reproduced with permission from Chen *et al.*, ACS Appl. Mater. Interfaces **10**, 9129 (2018). Copyright 2016 American Chemical Society.¹¹⁴ (c) Direct construction of SERS substrate on adhesive tapes for extraction of analytes and *in situ* SERS detection. In this strategy, the flexible adhesive tape-based SERS sensors can provide an affinity site for simultaneous sample collection and SERS analysis. Reproduced with permission from Jiang *et al.*, Anal. Chem. **88**, 2149 (2016). Copyright 2018 American Chemical Society.⁵⁷

tape are then transferred to the corresponding sensors to perform the subsequent assay.¹⁸² Tan *et al.* used adhesive tape modified with colorimetric indicators to quantify powder, by directly applying the adhesive tape to the analytes. Sampling cells (especially skin cells) using adhesive tapes is an appealing strategy for biomedical applications. Darvishi *et al.* used adhesive tapes to harvest the outermost cellular layers from a suspicious skin area and transferred the cells into a scanning electrochemical microscope.¹⁸³ This facile cell collection enabled by adhesive tapes was conducive to noninvasive melanoma detection.¹⁸⁴

The second strategy is the direct construction of sensing elements on adhesive tape and *in situ* analysis of the collected analytes. This method is widely used to fabricate flexible and sticky SERS sensors, where the adhesive tape provides an affinity site for plasmonic nano-materials (“hot spots”) by dip-coating¹⁸⁵ or transfer-printing strategies.^{186–188} These SERS tapes are still sticky after being modified with plasmonic materials that can further perform swab sampling tasks. Therefore, the functionalized SERS adhesive tapes provide direct extraction of analytes from the target objects without the assistance of organic solvent to wet the objective surfaces and maintain high SERS

activity.^{159,185} Chen *et al.* proposed a SERS tape that was fabricated by carefully and repeatedly dropping Au NPs solutions onto the sticky side of the adhesive tape until uniform SERS active substrate yielded.¹¹⁴ As a result, the SERS tapes enabled adhesively extracting pesticides (parathion-methyl) from diverse fruit and vegetable peels, including green vegetables, cucumbers, oranges, and apples [Fig. 8c], with high collection efficiency and convenience.¹⁸⁹

6. Stretch-release

Stretch-release is a unique manufacturing strategy that can only be done with stretchable and elastic material including elastic tape. In this process, target materials are first directly or indirectly (e.g., by transfer printing technique) constructed on a stretchable, elastic adhesive tape. When applying a certain stretching force to the elastic adhesive tape, deformation is formed in the target materials both parallel and perpendicular to the stretching direction caused by the Poisson effect.⁶ The target film is then compelled into an out-of-plane wavy microstructure after releasing stretched tape [Fig. 9(a)]. Both the stretchability and adhesion force of the elastic adhesive tapes play a

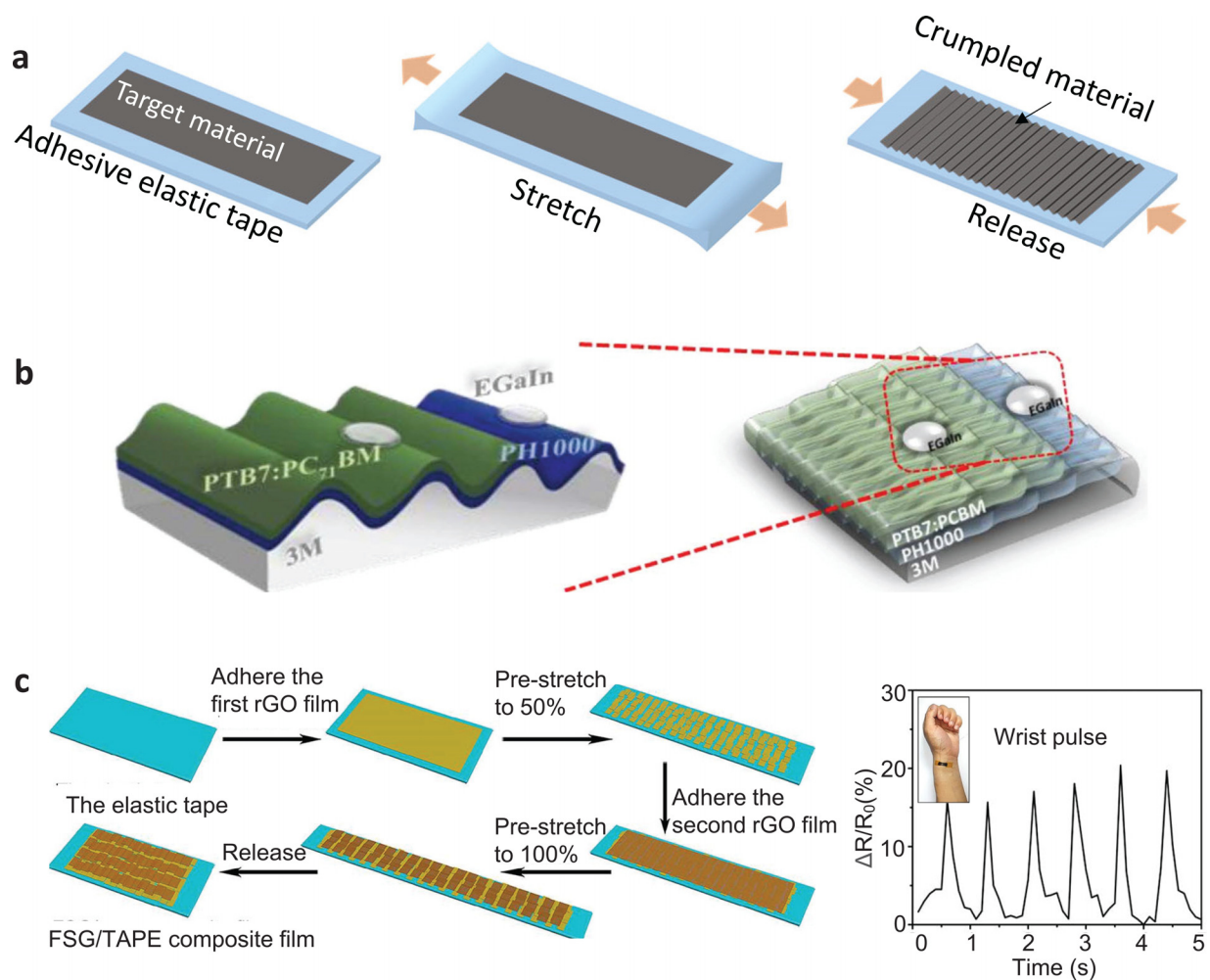


FIG. 9. Stretch-release. (a) Schematic of multiple wrinkle structures with mechanical stretchability and high specific surface area by stretch-release using elastic tapes. In this process, active material is first fabricated on a stretchable, elastic adhesive tape directly or indirectly. When applying a certain stretching force to the elastic adhesive tape, deformation is formed in the active layer and the active film is then compelled into a wavy microstructure after releasing stretched tape. (b) Fabrication of stretchable organic photovoltaics based on stretch-release technique using a 3MTM elastic tapes, and the device could maintain high power conversion efficiency (PCE) regardless of various mechanical measurement. Reproduced with permission from Chen *et al.*, *Sol. Energy Mater. Sol. Cells* **165**, 111 (2017). Copyright 2017 Elsevier.¹⁰³ (c) Construction of fish-scale-like graphene strain sensors based on a double stretching-release method using an elastic tape, where the presence of abundant wavy structures contribute to high sensitivity of the strain sensor. Reproduced with permission from Liu *et al.*, *ACS Nano* **10**, 7901 (2016). Copyright 2016 American Chemical Society.⁶

crucial role in the stretch-release operation. Stretchability is the prerequisite of the stretch-release technique, and adhesive force ensures tight contact between the target material layer and elastic tape without detachment.

There are two significant functions enabled by the stretch-release technique. First, it can be used to fabricate stretchable electronics capable of accommodating external force.⁶ A stretchable organic photovoltaic device based on 3MTM tape is demonstrated in Fig. 9(b).¹⁰³ In this work, a viscoelastic 3MTM VHB tape was pre-stretched and fixed onto a glass plate, and then sequentially spin-coated with PEDOT:PSS and organic heterojunction blend layer. The produced film was peeled off from the glass substrate and formed a buckle structure through the deposition of eutectic gallium–indium (EGaIn). This flexible and stretchable elastic tape-based photovoltaic battery achieved enhanced

power conversion efficiency (PCE, 30% greater than that of the corresponding PDMS-derived device), due to the improved uniformity of PEDOT:PSS film on tape. The device also showed stretchability that could maintain 80% of its original PCE regardless of 50 cycles of stretching at 20% strain. Second, the stretch-release can be used to fabricate buckled structures with high specific surface areas. The fabrication of these structures can be realized by other strategies, such as compression, molding, solvent swelling, thermal expansion, and 3D printing.¹⁹⁰ However, these strategies are complicated and time-consuming. By compression, stretch-release is relatively facile and can be repeated until enough wrinkles and fractures are created. Additionally, removing the elastic tape is also operable. Thus, the target material layer can be obtained in a freestanding manner.³⁴ Liu *et al.* applied an rGO film on a commercial elastic tape (VHB4910,

3MTM, Inc.), and the elastic tape was stretched to 50% so that cracks and fractures in the rGO layer were created. Then, another rGO film was attached to the first rGO layer and the elastic tape was further stretched to 100%. After released, a fish-scale-like rGO bilayer film was obtained [Fig. 9(c)].⁶ Due to the presence of abundant wavy structures, such a strain sensor realized high sensitivity (a gauge factor of 16.2–150) and low limit of detection (<0.1% strain), capable of tracking various human motions. Electrode and friction layers with high ratio surface areas are conducive to rich triboelectric charges for high-performance TENGs. Chen *et al.* proposed a crumpled graphene-based electrode of the TENG device.¹⁹¹ Here, the adhesive tape was biaxially pre-stretched and then relaxed along with the two pre-stretched directions. The TENG consisted of two layers: the bottom layer was crumpled/silicone film, where the crumpled graphene film acted as simultaneously electrode and friction layer; the top layer included silicone/planar graphene film, where the silicone and graphene served as a friction layer and the other electrode, respectively. Benefitting from the crumpled graphene with a successively wavy interface, this TENG could work in compressive, stretching, and hybridized modes, respectively, and its output voltage was higher than that of the TENG with planar graphene by one magnitude (compressive mode).

7. Bonding

Bonding is one of the most fundamental functions of adhesive tapes in daily life, such as fastening two pieces of paper together

(bonding between internal elements) and bonding a piece of paper on the wall (bonding with external elements). Similarly, for flexible electronics applications, adhesive tape-assisted bonding techniques can be divided into two types: one is bonding between internal items [Fig. 10(a)], sometimes, this bonding process is also called encapsulation, sealing, or packaging]. Sophisticated flexible electronics usually contain multivariate subsystems. Thus, rational assembly of these substructures into an entire system using adhesive tapes is of great significance to ensure complete and reliable functionalities.^{7,192,193} For example, it is necessary to keep these electronic elements away from the wet surface by encapsulating them in an independent room, otherwise, short circuit or inaccurate signal transmission will occur.¹⁹⁴ Li and co-workers utilized commercial Kapton tape as an adhesive encapsulation layer of perovskite solar cells.¹⁹⁵ The encapsulated cells maintained 96.3% of their initial PCE even underwater for 1620 s with continuous illumination, significantly improving the water resistance of perovskite solar cells for commercial applications. Conductive copper tapes have been simultaneously adopted as the encapsulation and electrode layer of perovskite solar cells.¹¹⁸ The conductive copper tape was heated to 70 °C so that the acrylic adhesive was softened and in close contact with the photoactive layer [Fig. 10(b)]. The PCE (measured within 240 h in a N₂ glovebox) of resulting perovskite solar cells was more stable than that with traditional thermally-evaporated Al electrodes. In another work, a facile TENG device was achieved using Kapton tape-based bonding technique, where the top and bottom electrodes were flexible ITO (coated on polyethylene terephthalate, PET)

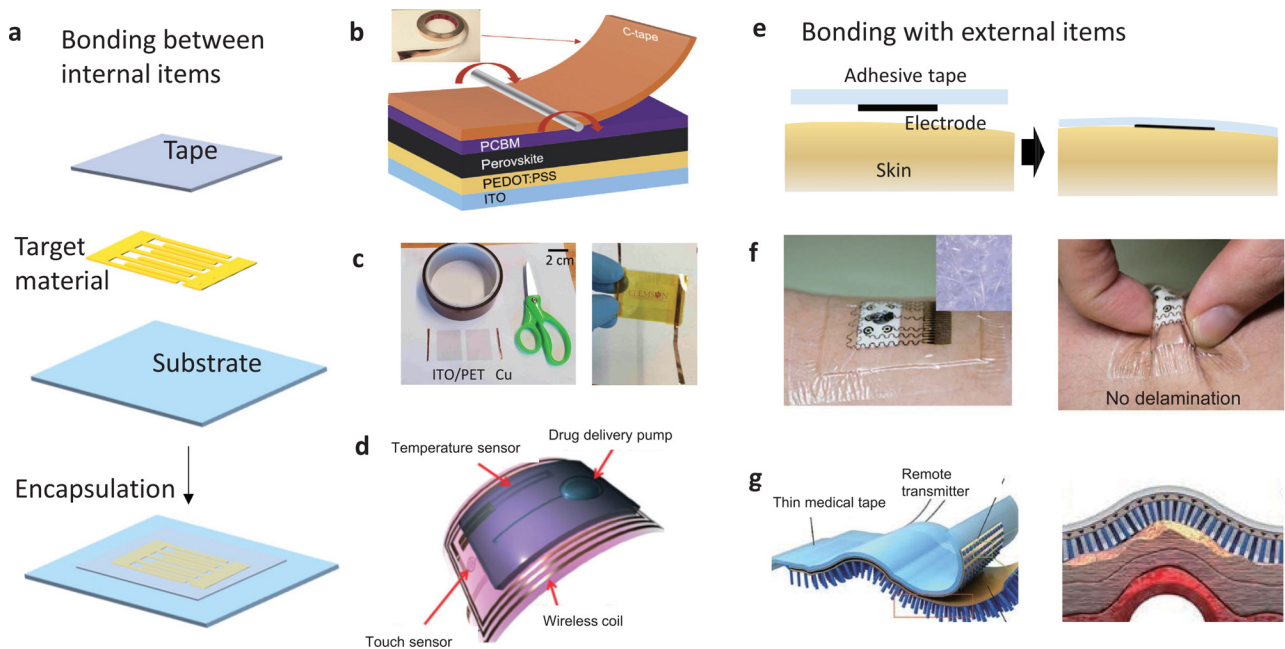


FIG. 10. Bonding. (a) Bonding between internal items using adhesive tapes for packaging individual layers of flexible electronics into a whole device. (b) Cu conductive tape as a simultaneous lamination layer and top electrode layer of perovskite solar cells. Reproduced with permission from Shao *et al.*, *Nano Energy* **16**, 47 (2015). Copyright 2015 Elsevier.¹¹⁸ (c) A facile TENG assembled by flexible ITO, Kapton tape, and Cu connecting wires. Reproduced with permission from Mallineni *et al.*, *Nano Energy* **35**, 263 (2017). Copyright 2017 Elsevier.¹³ (d) Kapton tape as a seal layer of microfluidic drug pumping patch. Reproduced with permission from Honda *et al.*, *Adv. Funct. Mater.* **29**, 15 (2019). Copyright 2014 Wiley-VCH.¹¹⁹ (e) Bonding adhesive tape-based electronics to external items such as human epidermis. (f) A waterproof tattoo-based sweat electronic patch capable of tight bonding on skin. Reproduced with permission from Lee *et al.*, *Sci. Adv.* **3**, e1601314 (2017). Copyright 2017 Authors, licensed under a Creative Commons Attribution (CC BY) license.¹³⁹ (g) A skin-conformal medical tape-based microhair pressure sensor for pulse signal monitoring. Reproduced with permission from Pang *et al.*, *Adv. Mater.* **27**, 634 (2015). Copyright 2015 Wiley-VCH.¹¹⁶

and Kapton tape-bonded flexible ITO [Fig. 10(c)], respectively.¹³ Kapton tape was selected here due to its relatively low rank in the triboelectric series (charge affinity: -70 nC J^{-1} , easily charged negatively) with relatively low compression modulus (2.5 GPa), and high compressive yield (150 MPa, eliminating plastic deformations at higher loads). The materials used in this TENG were so cheap ($\$0.06 \text{ cm}^{-2}$), which possessed a huge potential for industrial production. Bonding different layers in microfluidic electronics using adhesive tapes are crucial to ensure reliable capillary wicking of fluids and eliminate the leakage and cross-contamination between microchannels.^{196,197} Figure 10(d) illustrates a Kapton tape-encapsulated microfluidic drug delivery system.¹¹⁹ PDMS microfluidic chip was fabricated by soft lithography and strongly bonded onto a piece of Kapton tape. Touch/temperature sensors and wireless coils were configured on the Kapton tape, and dyed liquid mimicking a drug was loaded inside the PDMS microchamber. After imposing finger pressure, the drug could be on-demand ejected out from the microchamber to the target area.

Another adhesive tape-assisted bonding technique is bonding flexible devices to external items, especially human skin is a common external item. Bonding flexible electronics with the human epidermis has aroused plenty of wearable tape-on-skin devices [Fig. 10(e)]. These wearable devices are usually designed as a patch,¹⁹⁹ tattoo,⁴ or bandage style.^{17,200} Tight bonding with human skin is a prerequisite for epidermal electronics. In particular, for wearable sweat biosensors, given the damp skin microenvironment during sweating, reliable epidermal adhesion and mechanical stability are extremely essential.^{201–203} Adhesive tapes can serve as an epidermal adhesive layer, providing strong bonding between the sweat patch and sweaty epidermis.^{37,204–206} Porous medical adhesive tapes were widely adopted in a sweat microfluidic platform.¹¹ The biocompatible adhesives acrylic adhesive possessed good attachment and moisture vapor transmission rate (MVTR) ($2.08 \text{ mg/cm}^2 \text{ h}$) without any chemical or physical irritation to the skin. Lee *et al.* proposed a tape-based microneedles hybrid electronics as a simultaneous sweat sensor and transdermal drug (metformin) delivery patch [Fig. 10(f)].¹⁹⁸ Such a device included multiplex sensors (a graphene-based glucose sensor), a heater, and hyaluronic acid hydrogel microneedles coated with phase change materials. Once excessive sweat glucose was detected, the microneedle arrays were heated over critical temperature ($41\text{--}42^\circ\text{C}$) by the heater. As a result, the drug (metformin) loaded with phase change nanoparticles was thermos-responsively released into the bloodstream.²⁰⁷ Conformal skin adhesion plays a vital role in designing wearable pressure/strain sensors with low background noise for diverse applications including artificial e-skins, human-machine interface, and personalized diagnosis.^{77,208} A bioinspired microhairy pressure sensor based on medical tapes has been developed [Fig. 10(g)].¹¹⁶ The core sensing element consists of an Au-polyethylene naphthalene electrode with microhairy capacitive structure (to maximize the contact area between the sensors and the curved surface of the skin) on a medical tape. Here the medical tape greatly improved skin adaptability and biomedical compliance, ensuring the mechanical stability of the epidermal pressure sensor regardless of bending and deforming. In addition to human skin, adhesive tape-based devices can also be bonded with other external items. For instance, some researchers attached the as-prepared adhesive tape-based sensor on a disposable diaper,²⁰⁹ or a glove²¹⁰ for *in situ* biochemical analysis.

There has been a technique that directly applies the commercially available PSA (that is, no backing) on the top of flexible substrates for bringing the adhesive properties to flexible electronics.^{211,212} Such a bare PSA facilitates bonding between internal items of flexible electronics, as well as bonding the resulting adhesive flexible electronics on external items. Laminates integrated with a soft and low-modulus PSA have recently been introduced in foldable electronics to improve their mechanical reliability.²¹³ Rojer's group designed a skin-safe PSA-based sweat sensor, wherein the waterproof adhesives not only connected various device components (including microfluidic patch, color reference, NFC coil), but also provided strong bonding between the integrated sweat microfluidic electronics and volunteer's epidermis even underwater.³⁷

8. Additive techniques

When adhesive tape emerges as a bare substrate, it is of poor functionalities and cannot satisfy the demand for state-of-art electronic devices. Fortunately, adhesive tapes are amenable to be further modified due to their distinct sticky feature, which provides favorable affinity interaction toward the added functional elements. Recently, tremendous efforts have shifted to adding functional elements including conductors (e.g., metal, carbon, conductive polymers, and their derivatives), and semiconductors (e.g., metallic oxide). These functional elements serve as conductive paths, electrodes, or other components. We call these additive techniques in this paper. Here, we give several typical examples of these additive techniques, and the corresponding technical features, tape types, updated performances, and applications of the adhesive tape-based flexible electronics will be discussed in detail.

Screen printing is a common technique for fabricating electrodes or conductive tracks on adhesive tape substrates, where a blade or squeegee is moved across the screen to fill the open mesh apertures with printing ink. Carbon and metal inks (e.g., Au, Ag/AgCl) have been widely used in the construction of three/two-electrodes systems for electrochemical sensors [Fig. 11(a)],^{92,214} and chemical batteries¹⁶ on adhesive tapes by screen-printing. Wang's group designed a smart bandage with modified screen-printed electrodes (where polyaniline and solid Ag/AgCl served as the working electrode and reference electrode, respectively) for continuously monitoring wound pH based on the potentiometric transition.⁸⁴ Ink printing is another significant printing technique, where functional components can be deposited on adhesive tape in a quick, precise, reproducible, and mask-free manner. High-resolution inkjet printing on adhesive tape is a common strategy for flexible displays, electromechanical systems, and other microelectronic devices.²¹⁷ A graphene micro-supercapacitors was proposed based on a full inkjet printing technique, where both electrolytes [poly(4-styrenesulfonic acid)] and interdigitated electrodes (graphene inks) are printable. The inkjet printing is compatible with various substrates including Kapton tape in a scalable and massive manner [Fig. 11(b)].²¹⁵ Three-dimensional (3D) printing enables on-demand and direct printing of specific entities on adhesive tapes by layer-to-layer accumulation.⁹⁰ Huang's group reported 3D optoelectronic and sensing fibers, which were fabricated onto copper adhesive tape-based electrodes based on the 3D printing technique [Fig. 11(c)].¹¹³ First, the tip of the core-shell nozzle containing core solution (Ag or PEDOT:PSS) was placed above heated copper tape electrodes, allowing the pendant

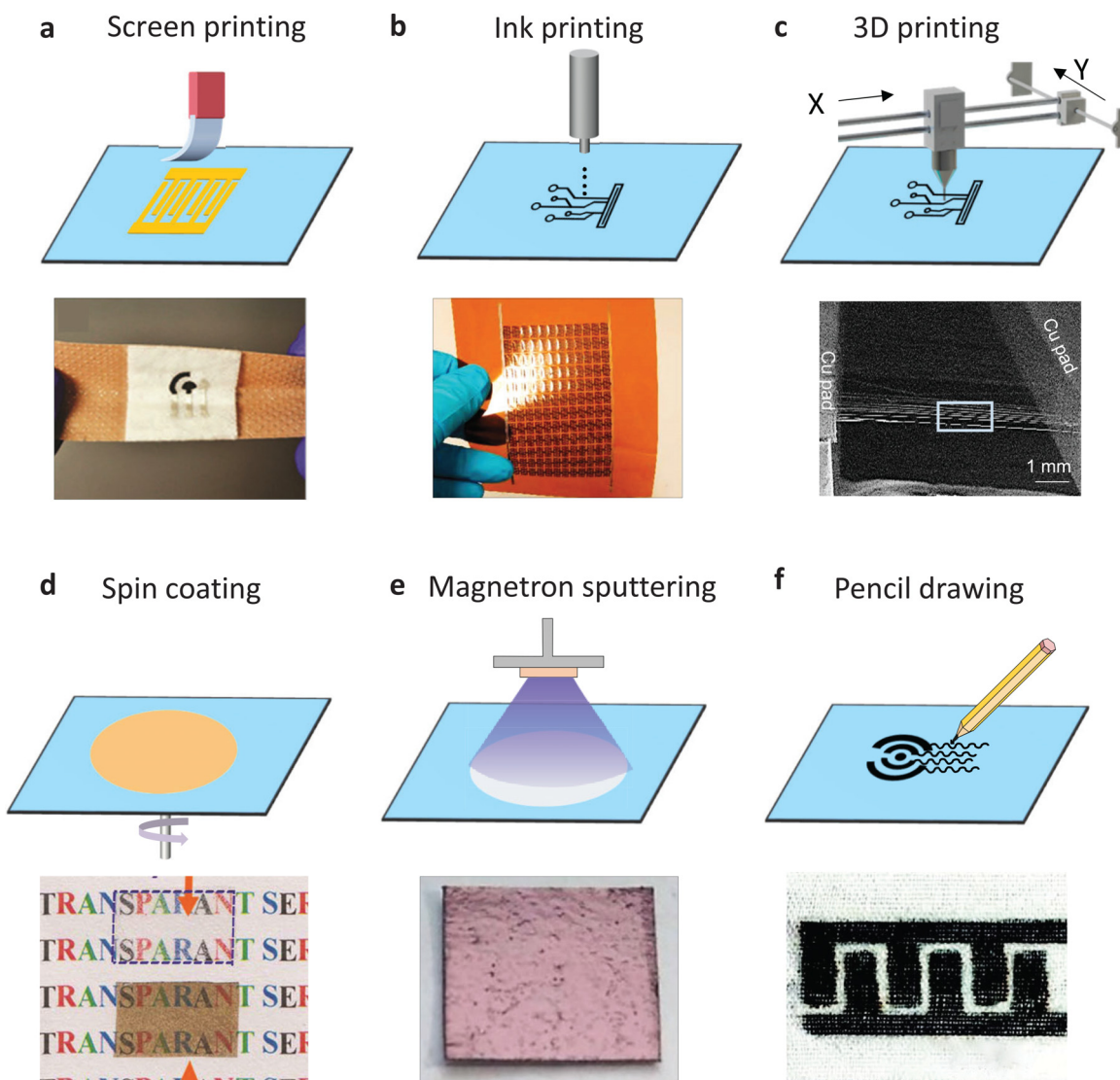


FIG. 11. Additive physical techniques related to adhesive tapes. (a) Screen printing of tyrosinase sensing electrode arrays on a medical tape. Reproduced with permission from Ciui *et al.*, *Adv. Healthcare Mater.* **7**, 1701264 (2018). Copyright 2018 Wiley-VCH.²¹⁴ (b) Scalable fabrication of graphene microsupercapacitors on a Kapton tape by ink printing. Reproduced with permission from Li *et al.*, *ACS Nano* **11**, 8249 (2017). Copyright 2017 American Chemical Society.²¹⁵ (c) Three-dimensional (3D) printed inflight fiber on copper adhesive tape toward optoelectronic and sensing architectures. Reproduced with permission from Wang *et al.*, *Sci. Adv.* **6**, eaba0931 (2020). Copyright 2020 Authors, licensed under a Creative Commons Attribution (CC BY) license.¹¹³ (d) Spin coating SiO_2 NWs on a Scotch tape as a precursor substrate for deposition of Ag NPs. Reproduced with permission from Liu *et al.*, *Nanoscale* **9**, 15901 (2017). Copyright 2017 Royal Society of Chemistry.¹²⁰ (e) CAT with magnetron-sputtered gold as an electrochemical sensing electrode for detection of heavy metals. Reproduced with permission from Sens. Actuators, B **236**, 218 (2016). Copyright 2016 Elsevier.²¹⁶ (f) Pencil drawing of flexible micro-supercapacitors on a medical tape. Reproduced with permission from Zhu *et al.*, *Small* **15**, 1804037 (2019). Copyright 2019 Wiley-VCH.³⁶

drop from the nozzle to be attached to the copper tape. The authors then repeated stage translations, during which the solution eventually solidified into parallel conducting fibers, bridging the suspension gap between two copper tapes. The 3D printed inflight fiber on copper tape electrode could act as a moisture flow sensor and noncontact respiratory sensor. The spin coating technique can be used to produce a relatively uniform film on adhesive tapes [Fig. 11(d)].²¹⁸ Liu *et al.* fabricated SiO_2 NWs on Scotch tape via spin coating strategy,¹²⁰ where the SiO_2 NWs solution was added to the center of tape substrate with

low or no spinning, and then rotated at high speed to spread the coating material through centrifugal force. The thickness of SiO_2 NWs could be controlled by repeating the time of spin coating. By further deposition of AgNPs on the SiO_2 NWs-coated Scotch tape, a highly active SERS substrate was obtained. Magnetron sputtering is a high-rate vacuum coating technique that allows the deposition of many types of materials on various substrates under a magnetic field. By magnetron sputtering, metallic films can be coated on the adhesive side as an electrode [Fig. 11(e)],²¹⁶ or transitional layer for further

physical and chemical modification.¹⁹ Surprisingly, the “pencil drawing” technique can also turn bare tape into advanced electronic devices. The “pencil” can be a compressed carbon pillar,⁸⁸ or a commercial pencil.^{36,219} When applying these pencils to draw across the rough/porous structures of the tape surface, graphitic is left and serves as the conductive component. This pencil drawing is perhaps the simplest and easiest strategy to improve the functionality of adhesive tapes. A skin-mountable micro-supercapacitor was prepared by pencil drawing on a medical tape. MnO₂ nanosheets were further deposited on the graphite trace after pencil drawing, by *in situ* redox reaction [Fig. 11(f)]. This bandage-like supercapacitor based on MnO₂/graphite electrodes could be conformably taped on the epidermis, and maintain stable capacitive features (over 90%) regardless of various physiological motions (200 bending cycles). Other additive techniques, such as dip-casting,²²⁰ roll-coating,²¹⁰ etc., have also been extensively investigated for adhesive tape-related flexible smart electronics. Materials fabricated by these single or hybrid physical approaches can remarkably expanding the functionalities of adhesive tape. It is competitive to develop rapid, facile, and low-cost physical techniques to enrich the electronic elements on adhesive tapes, which can greatly accelerate the update of flexible smart electronics from the laboratory to the commercial market.

9. Subtractive techniques

In contrast to adding components to adhesive tapes, the part of adhesive tapes (including the backings and PSAs) can be partially removed from the pristine one. We call this subtractive technique in this paper. The main aim of subtractive techniques is to create micropores or microchannels on adhesive tape by manual or laser cutting [Fig. 12(a)]. Manual cutting is quite easy using a knife or puncher. However, manual cutting is limited by low manufacturing efficiency and resolution. Instead, laser cutting can overcome these challenges and create delicate micro-nanostructures in a high-throughput manner.

The adhesive tapes after manual or laser cutting have three important roles in the construction of flexible electronics. First, as a template for the fabrication of patterned electronics. For example, by transferring a laser-cut adhesive layer on PDMS, high-resolution liquid alloy arrays were created with fine shape definition boundaries.¹⁶⁷ Mostafalu *et al.* illustrated a tape-based electrochemical wound oxygen sensor, where the core Ag and Zn electrodes were patterned on a flexible parylene-C substrate using laser-engraved tape as a template.⁹³ Song *et al.* fabricated carbon electrode arrays by vacuum filtration of CNTs on a poly(vinylidene fluoride) layer using the laser-cut tape as a template [Fig. 12(b)].²²¹ As a result, the shape and size of the electrode arrays could be on-demand designed in a scalable manner. An addressable 36-site electrochemical sensor was fabricated based on the tape-based template method. The addressable electrochemical sensor provided high-throughput screening of antioxidants on different vegetables and fruits. Second, as a fluid-wicking layer [Fig. 12(c)]. Adhesive tapes can also be used for microfluidics like traditional PDMS materials after manual or laser cutting techniques.^{18,61} The micropores and microchannels on adhesive tapes can define the opening for fluids inlet,¹¹ chamber for fluid storage,²²² and micro-channel for fluids flowing on adhesive tapes.²²³ Also, the punched micropores on adhesive tapes are conducive to draining the excessive biofluid, which can overcome the poor adhesion caused by the biofluid. Fraiwan *et al.*

illustrated a tape-paper hybrid biofuel cell (BFC).²²⁴ A piece of adhesive tape with a micropore served as both the acolyte sample input and device encapsulation layer. Gao's group presented a self-powered sweat sensor based on a sweat-based BFC module.³⁵ The sensing electrode and BFC were encapsulated by two layers of medical tapes and one layer of PDMS, forming a stacked sandwich structure (tape/PDMS/tape). The top medical tape layer and medium PDMS layer had individual laser-cut containers, where the configuration of BFC and sensing components could be accommodated, respectively. The bottom medical tape (skin adhesive layer) with laser-patterned openings reduced the area of occluded sweat glands by a quarter, avoiding compensatory effects during sweat secretion, which otherwise increased the local sweat rate due to occlusion of surrounding sweat glands.³⁷ Third, as a conductive pathway. Of course, this mainly refers to conductive tapes. Zhang's group employed a nickel-coated conductive tape to fabricate well-defined conductive routes by laser cutting [Fig. 12(d)]. The resulting conductive routes were transferred onto a flexible PET film and served as reference electrodes for wearable sweat sensing after being modified with Ag/AgCl ink.¹²² The same group also adopted a similar strategy to fabricate interdigital electrodes for an ultrasensitive wearable airflow sensor.²²⁵ Overall, this is a quite simple and universal technique to fabricate flexible and well-defined conductive tracks.²²⁵

B. Chemically-dominated techniques

1. Mechanochemical activation

As we mentioned earlier in Sec. IV A 1, peeling off adhesive tape from the backing creates charged species and radical species on the adhesive surface. The charged species contributed to triboelectrification, and the radical species play an important role in the fabrication/modifications of nanomaterials through a mechanochemical activation effect.²²⁶ An interesting research has shown that peeling off Scotch tape allows the direct fabrication of metallic nanoparticles.²⁷ Briefly, the PSA (adhesive side) of the Scotch tape was peeled off from the polyester backing and immersed into metal ion solutions [AgNO₃, HAuCl₄, PdCl₂, or Cu (acac)₂] for a few hours to several days. The resulting adhesive side gradually became a deep color, generating corresponding metal nanoparticles that were confirmed by microscopy and spectrum techniques. The potential mechanism could be attributed to the mechanoradicals arising from the homolytic cleavage of chemical bonds, which could *in situ* reduce metal ions to solid metals [Fig. 13(a)].^{124,227} Additionally, the peeling speed has an important impact on the radicals' amount. Higher peeling speed caused more radicals as well as more metallic nanoparticles. This simple strategy shows promising potential for the fabrication of metallic nanomaterials in resource-limited settings. Mechanical peeling off adhesive tapes from other surfaces (beyond the backing) can also result in reactive radicals on the interface. Lee *et al.* fabricated amorphous In-Ga-Zn-O (a-IGZO) thin-film transistors by combining mechanochemical activation and relatively mild thermal treatment [Fig. 13(b)].²²⁸ Mechanical stamping and pulling off the Scotch cellophane tapes from an a-IGZO transistor film generated abundant reactive radicals (O*) on the a-IGZO film surface. Thermal annealing was then performed to form metal-oxygen bonding and improve the reaction of O* radicals with vacancy sites.²²⁹ With this adhesive tape-based mechanochemical activation, the number of metal-oxygen bonding could be

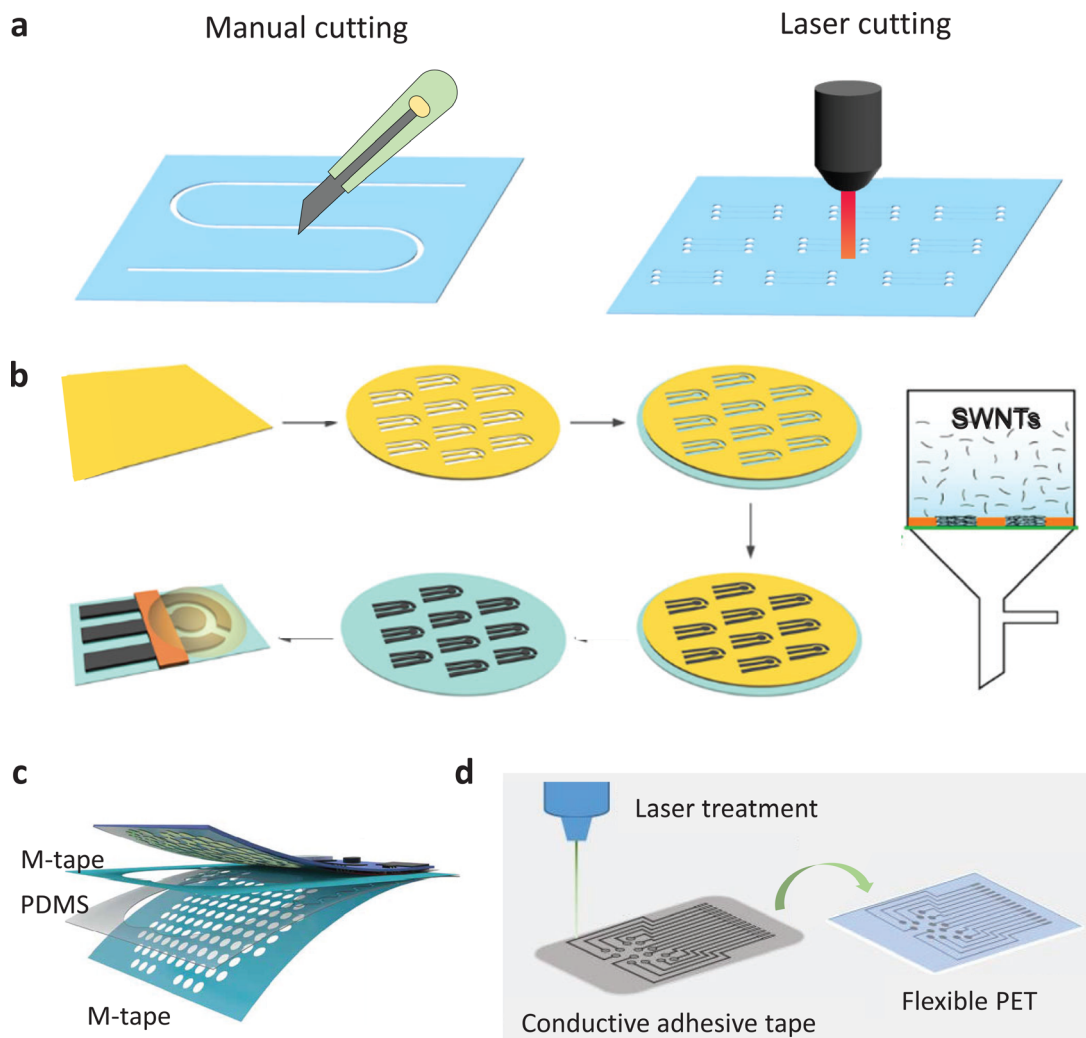


FIG. 12. Subtractive physical techniques related to adhesive tapes. (a) Schematic of micropores and micropatterns on adhesive tape created by manual and laser cutting techniques. (b) Electrochemical sensing arrays by vacuum filtration of CNTs on laser-cut adhesive tapes. Reproduced with permission from Song *et al.*, *ACS Sens.* **3**, 2518 (2018). Copyright 2018 American Chemical Society.²²¹ (c) Two pieces of laser-cut medical tapes as sweat inlets and a reservoir of sweat-based BCFs, respectively, for self-powered sweat microfluidic electronics. Reproduced with permission from Yu *et al.*, *Sci. Rob.* **5**, eaaz7946 (2020). Copyright 2020 American Association for the Advancement of Science.³⁵ (d) Laser-cut conductive adhesive tape as a flexible conductive path for design of sweat sensors. Reproduced with permission from He *et al.*, *Sci. Adv.* **5**, eaax0649 (2019). Copyright 2019 Authors, licensed under a Creative Commons Attribution (CC BY) license.¹²²

greatly improved and the number of defect sites could be reduced. As a result, the annealing temperature of the IGZO film significantly decreased (200 °C) compared to the conventional process (>300 °C). Additionally, the quality (e.g., mobility, on/off current ratio, and threshold voltage shift) of IGZO transistors film was also enhanced due to the improved carrier concentration via radical reactions.

2. Chemical deposition

Chemical deposition describes the stepwise growth of nanomaterials based on active seeds in a bottom-up manner. A wide variety of chemical deposition methods, such as chemical vapor deposition (CVD), chemical bath deposition (CBD), and electrodeposition can be

used to synthesize functional electronic elements with delicate micro/nanostructures on adhesive tapes as shown in Fig. 14(a).

CVD is usually performed under a gas atmosphere. Peeling adhesive tapes away from a specific substrate will leave adhesive residues on the substrate, more or less. Incredibly, it is these adhesive residues that can act as active seeds for CVD. Wang *et al.* showed that these adhesive seeds can participate in the nucleation or interruption during the growth of MoS₂ crystals [Fig. 14(b)] by inducing twinning as an impurity.²⁰ Briefly, a piece of adhesive tape was applied onto a SiO₂/Si substrate and then peeled off. Monolayer MoS₂ dendrites could stepwise grow on the peeled SiO₂/Si substrate via atmospheric pressure CVD under specific atmospheric pressure (8 sccm) and temperature (600 °C). The types of adhesive tape had a significant impact on the

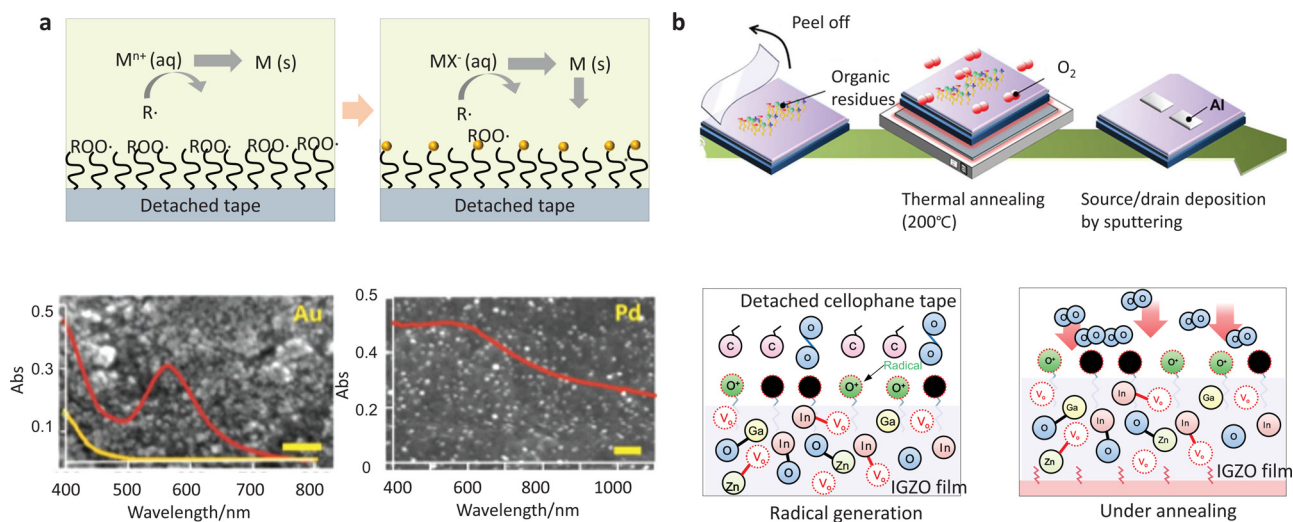


FIG. 13. Mechanochemical activation. (a) The schematic of mechanoradicals generated on the PSAs by pulling off adhesive tapes, capable of *in situ* reduction of metal ions to solid metal nanoparticles. The mechanoradicals are formed on detached tape (adhesive side), which function as reduction reagent capable of *in situ* reduction metal ions to solid metals. Reproduced with permission from Baytekin *et al.*, *J. Am. Chem. Soc.* **137**, 1726 (2015). Copyright 2015 American Chemical Society.²⁷ (b) Integrating mechanochemical and thermal annealing for fabrication of a-IGZO transistors film. Mechanochemical-activation-treated a-IGZO film with numerous radical species to reduce the required thermal annealing temperature. Compared to non-treated samples, the radical species originating from peeling off adhesive tapes significantly increase the metal-oxygen bonding under thermal annealing. Reproduced with permission from Lee *et al.*, *ACS Appl. Mater. Interfaces* **12**, 19123 (2020). Copyright 2020 American Chemical Society.²²⁸

MoS₂ morphology: when the substrate was treated with “Scotch[®] Transparent tape,” most MoS₂ showed irregular dendrites; however, when the substrate was modified with “Scotch[®] Magic[™] tape,” most MoS₂ exhibited dendrites with trigonal backbones. The reason could be that different adhesive compositions (impurity type) could induce different defects at both the initial nucleation stage and growth stage. Interestingly, heat treatment of conductive copper tape can generate graphene film [Fig. 14(c)].⁷¹ In this process, the conductive copper tape was preheated at 750 °C, during which the PSA contracted, volatile components evaporated and then remaining carbonaceous residues formed agglomerates on the copper foil, which served as a carbon source for the growth of graphene. When applying the mixed Ar/H₂ gas flow and increasing the temperature up to 1000 °C, volatile hydrocarbons could be created due to the interaction of H₂ and carbonaceous residues, providing a secondary carbon source for the growth of graphene in a CVD-like process. CBD is another common method for the deposition of metal chalcogenide/oxide thin films. Sometimes, CBD is also called solution growth, controlled precipitation, or simply chemical deposition. Hassan *et al.* fabricated plenty of well-aligned vertical ZnO NRs on Kapton tape by CBD, on which Pd NPs were introduced using the magnetron sputtering technique for fast UV detection and hydrogen sensing.³⁸ Deng *et al.* proposed a wearable self-powered piezoelectric pressure sensor by hydrothermal deposition of ordered ZnO NRs on Kapton tape.²³⁰

Electrodeposition is a rapid deposition method for the preparation of metal nanomaterials on an electrode interface and is usually carried out in an electrolyte solution.²³¹ However, considering the weak conductivity of most bare adhesive tapes, pretreatment techniques such as spin coating¹²⁰ magnetron sputtering^{17,54} transfer printing¹¹² of electronic components on these bare adhesive tapes are essential before electrodeposition. Zhang’s group fabricated Au NDs

by integrating magnetron sputtering and electrodeposition.¹⁹ The CAT was first sputtered with a layer of well-defined planar Au film via a customized photomask. Next, the gold-coated CAT, Ag/AgCl wire, and Pt wire served as the working electrode, reference electrode, and counter electrode, respectively, for the electrodeposition of the Au NDs on the planar Au sites. The Au NDs possess rich “hot-spots” and strong capillary force for capturing microdroplets, capable of on-site sensing of aqueous food contaminants. Based on this strategy, the same group also fabricated Au NDs on adhesive tape as sweat-sensing electrode arrays [Fig. 14(d)].¹⁷ Upon conformably taped on the sweaty skin, the hierarchical microstructure in Au NDs electrodes remarkably improved the electrochemical response signal compared to bare Au film, enabling highly sensitive and multiple sweat electrochemical sensing (glucose, lactate, Na⁺, and K⁺). Soni *et al.* proposed a Scotch tape-based supercapacitor by combining transfer printing and electrodeposition.¹¹² Briefly, an ultrathin Grafoil sheet (74 μm in thickness) was transferred onto a Scotch tape, followed by electrodeposition of grass-like MnO₂ thin films. The porous and grass-like structure of the MnO₂ facilitated electrolyte penetration, exhibiting low equivalent series resistance (7 Ω), high specific capacitance (776 F g⁻¹ at 0.5 A g⁻¹ current density), and volumetric capacitance (2.0 F cm⁻³).

V. OUTLOOK AND CONCLUSION

The past few decades have witnessed growing research interest in adhesive tape-enabled flexible electronics from a single material to integrated systems. In this review, we highlighted the significant progress of flexible electronics enabled by adhesive tapes. The unique sticky feature of adhesive tapes has brought new possibilities for flexible electronics to be passively used as supporting substrates of flexible electronics and to actively construct functional components of flexible electronics, both of which have contributed to diverse applications.

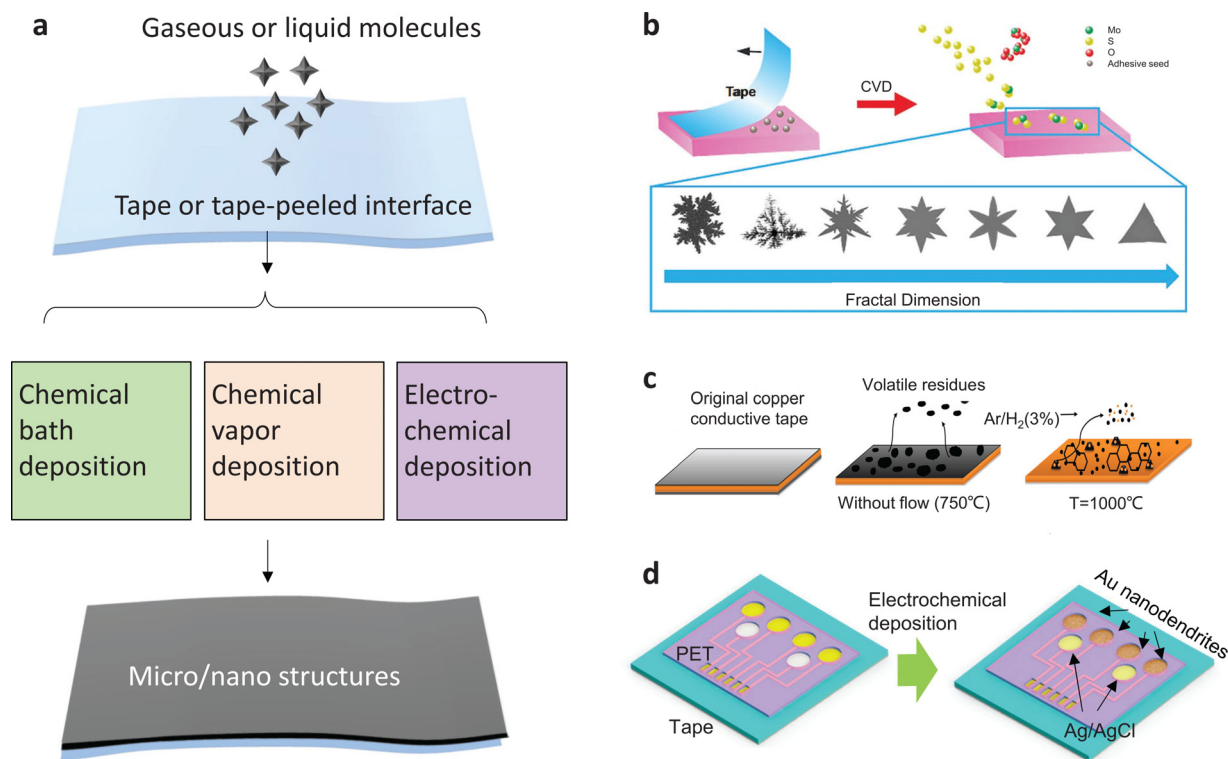


FIG. 14. Chemical deposition. (a) Micro/nanostructures on adhesive tape or tape-treated interface by chemical vapor deposition, chemical bath deposition, and electrodeposition. (b) Deposition of MoS₂ dendrites on the adhesive tape-peeled SiO₂/Si substrate based on the CVD technique. Reproduced with permission from Wang *et al.*, ACS Nano **12**, 635 (2018). Copyright 2018 American Chemical Society.²⁰ (c) Schematic of the growth mechanism of graphene on copper adhesive tape under heat treatment. Reproduced with permission from J. Mater. Sci. **52**, 4356 (2017). Copyright 2017 Springer.⁷¹ (d) Electrodeposition of Au NDs on a CAT as sweat sensing electrode arrays. Reproduced with permission from He *et al.*, ACS Sens. **5**, 1548 (2020). Copyright 2020 American Chemical Society.¹⁷

Despite these signs of progress, in general, the correlative exploration of tape-enabled flexible electronics is in the early stage, and several major challenges in terms of material library, device stability, scaling commercialization, etc., remain in the following aspects:

- (1) Mechanisms: Generally, the current understanding of the mechanism involving the adhesion model, free radicals/charged species during peeling off the tape, is immature. For example, there are many crude assumptions in the proposed model of adhesive mechanism (Sec. II B) and parallel plate capacitor (Sec. IV A 1). Therefore, these equations are capable of providing qualitative analysis instead of quantitative calculations of peel force and output voltage, respectively. More experiments using different types of adhesive tapes are also necessary to further validate the universality of these proposed models. Deep mechanism research may help us reveal the nanostructure–property–performance relationship of adhesive tapes and related flexible devices.
- (2) Fabrication techniques: most existing manufacturing techniques, including mechanical exfoliation, transfer printing, pencil drawing techniques, etc., are essentially trial-and-error processes lacking commercialized scalability. Given the final commercialization of flexible electronics, these methods should be

large-scale and high-throughput and only by this way, these adhesive tape electronics can be transformed from the laboratory to the commercial market. Taking the Scotch tape method as an example, although it is a facile, convenient, low-cost, and easy-to-operate strategy to fabricate single/few-layer 2D materials in a laboratory, the low yield and time consumption limit are its industrial output. Therefore, more efforts should be paid to developing large-scale and standardized fabrication techniques, bridging the gap between fundamental research and commercialization.

- (3) Physiological comfort and biocompatibility: Generally, the physiological comfort and biocompatibility of most adhesive tapes are weak, especially for on-body or *in vivo* applications. Unlike other flexible substrates with porous structures (e.g., fiber), the breathability of most adhesive tapes is a questionable issue. A medical tape is an ideal candidate; however, the adhesion of the regular medical tape is relatively weak, which may become invalid and delaminated from the body during long-term application. Additionally, functionalized devices based on adhesive tapes with good biocompatibility and biodegradability is urgently needed and will greatly accelerate the development of implantable electronics.²³² Natural protein-type adhesive tapes lay a solid foundation for the further development of

flexible implantable electronics. Some protein-derived adhesives have been proposed for flexible implantable electronics;^{233–235} however, these self-design adhesive materials have not been commercialized yet. Commercially available fibrin glue may be applicable for implantable electronics; unfortunately, their functionality is currently limited to fundamental medical adhesion (such as hemostasis, wound healing, and tissue adhesion).⁴¹ In other words, there is still a huge room to integrate commercial and biocompatible adhesive tapes for flexible implantable electronics (e.g., organ patches, neural electrodes, and brain-machine interfaces).

- (4) Integrated multifunctionalities: Integrated flexible electronic systems with multifunctionalities are of great value, such as multimodal sensing units, feedback therapy, and self-powered biosensing platforms.⁵ For example, adhesive tape-based therapeutic electronics simultaneously configured with sensors, actuators, and algorithms modules will improve our understanding of the relationship between disease and abnormal physiological signals. The development of multifunctional flexible devices based on adhesive tapes is relatively rare, since it is challenging to arrange multiple electronic elements together on a single piece of adhesive tape. The integrated system should be carefully designed to minimize the interfacial mismatch between each component. Additionally, rational data processing and logic algorithms (e.g., machine learning) are also essential to extract the data characteristics from different electronic modules.

It is anticipated that the new age of adhesive tape-enabled flexible electronics will advent upon all the upgrades and progress has finished. We hope that this review will facilitate researchers and engineers with more interest in the study of flexible electronics enabled by adhesive tapes and make more contributions to modern society.

ACKNOWLEDGMENTS

We acknowledge funding from Joint Fund of the Ministry of Education for Equipment Pre-research (No. 8091B0206), Shenzhen Stability Support Plan (No. 20200806163622001), Shenzhen Overseas Talent Program, and Shenzhen Key Laboratory for Nano-Biosensing Technology (No. ZDSYS20210112161400001).

AUTHOR DECLARATIONS

Conflict of Interest

The authors have no conflicts to disclose.

Author Contributions

Xuecheng He: Investigation (lead); Writing – original draft (lead). **Wenyu Wang:** Writing – review & editing (equal). **Shijie Yang:** Conceptualization (equal); Investigation (equal); Writing – review & editing (equal). **Feilong Zhang:** Writing – review & editing (supporting). **Zhen Gu:** Writing – review & editing (supporting). **Bing Dai:** Writing – review & editing (supporting). **Tailin Xu:** Conceptualization (lead); Funding acquisition (lead); Supervision (lead). **Yan Yan Shery Huang:** Writing – review & editing (lead). **Xueji Zhang:** Funding acquisition (equal); Supervision (equal); Writing – review & editing (equal).

DATA AVAILABILITY

Data sharing is not applicable to this article as no new data were created or analyzed in this study.

REFERENCES

- See https://www.scotchbrand.com/3M/en_US/scotch-brand/about/ for About Scotch Brand.
- Z. Ma, Q. Huang, Q. Xu, Q. Zhuang, X. Zhao, Y. Yang, H. Qiu, Z. Yang, C. Wang, Y. Chai, and Z. Zheng, *Nat. Mater.* **20**, 859 (2021).
- S. Liu, D. S. Yang, S. Wang, H. Luan, Y. Sekine, J. B. Model, A. J. Aranyosi, R. Ghaffari, and J. A. Rogers, *EcoMat* **4**, e12270 (2022).
- D. H. Kim, N. Lu, R. Ma, Y. S. Kim, R. H. Kim, S. Wang, J. Wu, S. M. Won, H. Tao, A. Islam, K. J. Yu, T. I. Kim, R. Chowdhury, M. Ying, L. Xu, M. Li, H. J. Chung, H. Keum, M. McCormick, P. Liu, Y. W. Zhang, F. G. Omenetto, Y. Huang, T. Coleman, and J. A. Rogers, *Science* **333**, 838 (2011).
- J. R. Sempionatto, M. Lin, L. Yin, E. De la Paz, K. Pei, T. Sona-Ard, A. N. de Loyola Silva, A. A. Khorshed, F. Zhang, N. Tostado, S. Xu, and J. Wang, *Nat. Biomed. Eng.* **5**, 737 (2021).
- Q. Liu, J. Chen, Y. R. Li, and G. Q. Shi, *ACS Nano* **10**, 7901 (2016).
- Y. Shi, F. Wang, J. Tian, S. Li, E. Fu, J. Nie, R. Lei, Y. Ding, X. Chen, and Z. L. Wang, *Sci. Adv.* **7**, eabe2943 (2021).
- D. Son, J. Lee, S. Qiao, R. Ghaffari, J. Kim, J. E. Lee, C. Song, S. J. Kim, D. J. Lee, S. W. Jun, S. Yang, M. Park, J. Shin, K. Do, M. Lee, K. Kang, C. S. Hwang, N. Lu, T. Hyeon, and D. H. Kim, *Nat. Nanotechnol.* **9**, 397 (2014).
- M. R. Prausnitz, S. Mitragotri, and R. Langer, *Nat. Rev. Drug Discovery* **3**, 115 (2004).
- J. Kim, J. R. Sempionatto, S. Imani, M. C. Hartel, A. Barfidokht, G. Tang, A. S. Campbell, P. P. Mercier, and J. Wang, *Adv. Sci.* **5**, 1800880 (2018).
- A. Koh, D. Kang, Y. Xue, S. Lee, R. M. Pielak, J. Kim, T. Hwang, S. Min, A. Banks, P. Bastien, M. C. Manco, L. Wang, K. R. Ammann, K. I. Jang, P. Won, S. Han, R. Ghaffari, U. Paik, M. J. Slepian, G. Balooch, Y. Huang, and J. A. Rogers, *Sci. Transl. Med.* **8**, 366ra165 (2016).
- L. B. Baker, J. B. Model, K. A. Barnes, M. L. Anderson, S. P. Lee, K. A. Lee, S. D. Brown, A. J. Reimel, T. J. Roberts, R. P. Nuccio, J. L. Bon Signore, C. T. Ungaro, J. M. Carter, W. Li, M. S. Seib, J. T. Reeder, A. J. Aranyosi, J. A. Rogers, and R. Ghaffari, *Sci. Adv.* **6**, eabe3929 (2020).
- S. S. K. Mallineni, H. Behlow, Y. C. Dong, S. Bhattacharya, A. M. Rao, and R. Podila, *Nano Energy* **35**, 263 (2017).
- C. G. Camara, J. V. Escobar, J. R. Hird, and S. J. Putterman, *Nature* **455**, 1089 (2008).
- S. Q. Ling, Y. Luo, L. Luan, Z. W. Wang, and T. Z. Wu, *Sens. Actuators, B* **235**, 732 (2016).
- S. Berchmans, A. J. Bandodkar, W. Jia, J. Ramirez, Y. S. Meng, and J. Wang, *J. Mater. Chem. A* **2**, 15788 (2014).
- X. He, S. Yang, Q. Pei, Y. Song, C. Liu, T. Xu, and X. Zhang, *ACS Sens.* **5**, 1548 (2020).
- X. Cheng, B. Wang, Y. Zhao, H. Hojajji, S. Lin, R. Shih, H. Lin, S. Tamayosa, B. Ham, P. Stout, K. Salahi, Z. Wang, C. Zhao, J. Tan, and S. Emaminejad, *Adv. Funct. Mater.* **30**, 1908507 (2019).
- X. He, S. Yang, T. Xu, Y. Song, and X. Zhang, *Biosens. Bioelectron.* **152**, 112013 (2020).
- J. Wang, X. Cai, R. Shi, Z. Wu, W. Wang, G. Long, Y. Tang, N. Cai, W. Ouyang, P. Geng, B. N. Chandrashekar, A. Amini, N. Wang, and C. Cheng, *ACS Nano* **12**, 635 (2018).
- W. Zeng, L. Shu, Q. Li, S. Chen, F. Wang, and X.-M. Tao, *Adv. Mater.* **26**, 5310 (2014).
- B. Wang and A. Facchetti, *Adv. Mater.* **31**, 1901408 (2019).
- Y. Zhang, L. Zhang, K. Cui, S. Ge, X. Cheng, M. Yan, J. Yu, and H. Liu, *Adv. Mater.* **30**, 1801588 (2018).
- H. Tai, Z. Duan, Y. Wang, S. Wang, and Y. Jiang, *ACS Appl. Mater. Interfaces* **12**, 31037 (2020).
- K. S. Novoselov, A. K. Geim, S. V. Morozov, D. Jiang, Y. Zhang, S. V. Dubonos, I. V. Grigorieva, and A. A. Firsov, *Science* **306**, 666 (2004).
- C. H. Lee, D. R. Kim, and X. L. Zheng, *Proc. Natl. Acad. Sci. U.S.A.* **107**, 9950 (2010).

- ²⁷H. T. Baytekin, B. Baytekin, S. Huda, Z. Yavuz, and B. A. Grzybowski, *J. Am. Chem. Soc.* **137**, 1726 (2015).
- ²⁸J. Ogawa, S. Fukui, K. Yoshino, Y. Suzuki, and S. Torigata, *IEEE Trans. Appl. Supercond.* **29**, 9001204 (2019).
- ²⁹N. Raravikar, A. Dobos, E. Narayanan, T. S. P. Grandhi, S. Mishra, K. Rege, and M. Goryll, *ACS Appl. Mater. Interfaces* **9**, 3554 (2017).
- ³⁰J. Gong, B. Xu, Y. Yang, M. Wu, and B. Yang, *Adv. Mater.* **32**, 1907948 (2020).
- ³¹F. K. Perkins, A. L. Friedman, E. Cobas, P. M. Campbell, G. G. Jernigan, and B. T. Jonker, *Nano Lett.* **13**, 668 (2013).
- ³²L. Wang, P. Chen, Y. C. Wang, G. S. Liu, C. Liu, X. Xie, J. Z. Li, and B. R. Yang, *ACS Appl. Mater. Interfaces* **10**, 16596 (2018).
- ³³S. Oren, H. Ceylan, P. S. Schnable, and L. Dong, *Adv. Mater. Technol.* **2**, 1700223 (2017).
- ³⁴J. S. Xu, J. Chen, M. Zhang, J. D. Hong, and G. Q. Shi, *Adv. Electron. Mater.* **2**, 1600022 (2016).
- ³⁵Y. Yu, J. Nassar, C. Xu, J. Min, Y. Yang, A. Dai, R. Doshi, A. Huang, Y. Song, R. Gehlhar, A. D. Ames, and W. Gao, *Sci. Rob.* **5**, eaaz7946 (2020).
- ³⁶S. Zhu, Y. Li, H. Zhu, J. Ni, and Y. Li, *Small* **15**, 1804037 (2019).
- ³⁷J. T. Reeder, J. Choi, Y. Xue, P. Gutruf, J. Hanson, M. Liu, T. Ray, A. J. Bandodkar, R. Avila, W. Xia, S. Krishnan, S. Xu, K. Barnes, M. Pahnke, R. Ghaffari, Y. Huang, and J. A. Rogers, *Sci. Adv.* **5**, eaau6356 (2019).
- ³⁸J. J. Hassan, M. A. Mahdi, S. J. Kasim, N. M. Ahmed, H. Abu Hassan, and Z. Hassan, *Mater. Sci.-Pol.* **31**, 180 (2013).
- ³⁹S. Nam and D. Mooney, *Chem. Rev.* **121**, 11336 (2021).
- ⁴⁰L. Wang, T. Xu, and X. Zhang, *TrAC, Trends Anal. Chem.* **134**, 116130 (2021).
- ⁴¹T. E. MacGillivray, *J. Card. Surg.* **18**, 480 (2003).
- ⁴²J.-W. Seo, H. Kim, K. Kim, S. Q. Choi, and H. J. Lee, *Adv. Funct. Mater.* **28**, 1800802 (2018).
- ⁴³H. E. Jeong and K. Y. Suh, *Nano Today* **4**, 335 (2009).
- ⁴⁴S. Baik, J. Lee, E. J. Jeon, B. Y. Park, D. W. Kim, J. H. Song, H. J. Lee, S. Y. Han, S. W. Cho, and C. Pang, *Sci. Adv.* **7**, eabf5695 (2021).
- ⁴⁵H. Lee, D. S. Um, Y. Lee, S. Lim, H. J. Kim, and H. Ko, *Adv. Mater.* **28**, 7457 (2016).
- ⁴⁶S. Wang, H. Luo, C. Linghu, and J. Song, *Adv. Funct. Mater.* **31**, 2009217 (2020).
- ⁴⁷Z. Ma, C. Bourquard, Q. Gao, S. Jiang, T. De Iure-Grimmel, R. Huo, X. Li, Z. He, Z. Yang, G. Yang, Y. Wang, E. Lam, Z. H. Gao, O. Supponen, and J. Li, *Science* **377**, 751 (2022).
- ⁴⁸S. Mapari, S. Mestry, and S. T. Mhaske, *Polym. Bull.* **78**, 4075 (2020).
- ⁴⁹See [http://www.pstc.org/44a/pages/index.cfm?pageID=3336\(1pp\)](http://www.pstc.org/44a/pages/index.cfm?pageID=3336(1pp)) for “Anonymous. Glossary of terms. Test methods for pressure sensitive adhesive tapes. Pressure Sensitive Adhesive Tape Council, 1996” (accessed October 2014).
- ⁵⁰M. M. Feldstein and R. A. Siegel, *J. Polym. Sci. B: Polym. Phys.* **50**, 739 (2012).
- ⁵¹V. Danilowska, P. Carretero, R. Tomovska, and J. M. Asua, *Polymer* **55**, 5050 (2014).
- ⁵²K. Takahashi, F. Yanai, K. Inaba, K. Kishimoto, Y. Kozono, and T. Sugizaki, *Langmuir* **37**, 11457 (2021).
- ⁵³F. London, *Trans. Faraday Soc.* **33**, 8b (1937).
- ⁵⁴J. N. Israelachvili, *Intermolecular and Surface Forces* (Academic Press, 2011).
- ⁵⁵Z. Gu, S. Li, F. Zhang, and S. Wang, *Adv. Sci.* **3**, 1500327 (2016).
- ⁵⁶See https://technicaldatasheets.3m.com/en_US?pfid=835 for Technical Dataheet, 3M™ Scotch® Cellophane Film Tape 610.
- ⁵⁷J. Jiang, S. Zou, L. Ma, S. Wang, J. Liao, and Z. Zhang, *ACS Appl. Mater. Interfaces* **10**, 9129 (2018).
- ⁵⁸K. Kim, H. Yu, J. Koh, J. H. Shin, W. Lee, and Y. Park, *Opt. Lett.* **41**, 1837 (2016).
- ⁵⁹L. Qiao, M. Benzigar, A. Subramony, N. Lovell, and G. Liu, *ACS Appl. Mater. Interfaces* **30**, 34337 (2020).
- ⁶⁰See https://technicaldatasheets.3m.com/en_US?pfid=431 for M. D. C. T. Technical Datasheet.
- ⁶¹H. Y. Y. Nyein, M. Bariya, L. Kivimaki, S. Uusitalo, T. S. Liaw, E. Jansson, C. H. Ahn, J. A. Hangasky, J. Zhao, Y. Lin, T. Happonen, M. Chao, C. Liedert, Y. Zhao, L. C. Tai, J. Hiltunen, and A. Javey, *Sci. Adv.* **5**, eaaw9906 (2019).
- ⁶²E. B. Secor, T. Z. Gao, A. E. Islam, R. Rao, S. G. Wallace, J. Zhu, K. W. Putz, B. Maruyama, and M. C. Hersam, *Chem. Mater.* **29**, 2332 (2017).
- ⁶³G. Hong, M. Zhou, R. Zhang, S. Hou, W. Choi, Y. S. Woo, J.-Y. Choi, Z. Liu, and J. Zhang, *Angew. Chem. Int. Ed.* **50**, 6819 (2011).
- ⁶⁴S. Seok, H. Park, and J. Kim, *Micromachines* **11**, 605 (2020).
- ⁶⁵J. Liang, Y. Ma, F. Wang, and W. Yang, *Chem. Mater.* **22**, 4254 (2010).
- ⁶⁶See https://www.kaptontape.com/1_Mil_Kapton_Tapes_Datasheet.php for M. K. T. Technical Datasheet.
- ⁶⁷R. Melik, E. Unal, N. K. Perkgoz, C. Puttlitz, and H. V. Demir, *Appl. Phys. Lett.* **95**, 181105 (2009).
- ⁶⁸R. R. Ghimire and A. K. Raychaudhuri, *Appl. Phys. Lett.* **110**, 052105 (2017).
- ⁶⁹P. Bai, G. Zhu, Y. S. Zhou, S. Wang, J. Ma, G. Zhang, and Z. L. Wang, *Nano Res.* **7**, 990 (2014).
- ⁷⁰M. Liu, X. Pu, C. Jiang, T. Liu, X. Huang, L. Chen, C. Du, J. Sun, W. Hu, and Z. L. Wang, *Adv. Mater.* **29**, 1703700 (2017).
- ⁷¹J. J. Vivas-Castro, G. Rueda-Morales, G. Ortega-Cervantez, L. A. Moreno-Ruiz, and J. Ortiz-Lopez, *J. Mater. Sci.* **52**, 4356 (2017).
- ⁷²S. Pasche, S. Angeloni, R. Ischer, M. Liley, J. Luprano, and G. Voirin, *Adv. Sci. Technol. Res. J.* **57**, 80 (2008).
- ⁷³Z. Wang, T. Liu, L. Jiang, M. Asif, X. Qiu, Y. Yu, F. Xiao, and H. Liu, *ACS Appl. Mater. Interfaces* **11**, 32310 (2019).
- ⁷⁴S. W. Lee, W. Lee, D. Lee, Y. Choi, W. Kim, J. Park, J. H. Lee, G. Lee, and D. S. Yoon, *Sens. Actuators, B* **266**, 485 (2018).
- ⁷⁵Y. Chu, J. Zhong, H. Liu, Y. Ma, N. Liu, Y. Song, J. Liang, Z. Shao, Y. Sun, Y. Dong, X. Wang, and L. Lin, *Adv. Funct. Mater.* **28**, 1803413 (2018).
- ⁷⁶X. M. Wang, L. Q. Tao, M. Yuan, Z. P. Wang, J. Yu, D. Xie, F. Luo, X. Chen, and C. Wong, *Nat. Commun.* **12**, 1776 (2021).
- ⁷⁷B. Yin, X. Liu, H. Gao, T. Fu, and J. Yao, *Nat. Commun.* **9**, 5161 (2018).
- ⁷⁸X. Zhang, Y. Jing, Q. Zhai, Y. Yu, H. Xing, J. Li, and E. Wang, *Anal. Chem.* **90**, 11780 (2018).
- ⁷⁹N. Sooin, P. Zhao, K. Prashanthi, J. Chen, P. Ding, E. Zhou, T. Shah, S. C. Ray, C. Tsonos, T. Thundat, E. Siores, and J. Luo, *Nano Energy* **30**, 470 (2016).
- ⁸⁰L. Shi, S. R. Dong, P. Ding, J. K. Chen, S. T. Liu, S. Y. Huang, H. S. Xu, U. Farooq, S. M. Zhang, S. J. Li, and J. K. Luo, *Nano Energy* **55**, 548 (2019).
- ⁸¹C. J. Lim, S. Lee, J. H. Kim, H. J. Kil, Y. C. Kim, and J. W. Park, *ACS Appl. Mater. Interfaces* **10**, 41026 (2018).
- ⁸²J. M. Karp and R. Langer, *Nature* **477**, 42 (2011).
- ⁸³F. Tehrani, H. Teymourian, B. Wuerstle, J. Kavern, R. Patel, A. Furnidge, R. Aghavali, H. Hosseini-Toudeshki, C. Brown, F. Zhang, K. Mahato, Z. Li, A. Barfidokht, L. Yin, P. Warren, N. Huang, Z. Patel, P. P. Mercier, and J. Wang, *Nat. Biomed. Eng.* **6**, 1214 (2022).
- ⁸⁴T. Guinovart, G. Valdés-Ramírez, J. R. Windmiller, F. J. Andrade, and J. Wang, *Electroanalysis* **26**, 1345 (2014).
- ⁸⁵X. Sun, M. Dong, Z. Guo, H. Zhang, J. Wang, P. Jia, T. Bu, Y. Liu, L. Li, and L. Wang, *Int. J. Biol. Macromol.* **167**, 10 (2021).
- ⁸⁶R. D. Boehm, B. Chen, S. D. Gittard, B. N. Chichkov, N. A. Monteiro-Riviere, A. Nasir, and R. J. Narayan, *J. Adhes. Sci. Technol.* **28**, 387 (2012).
- ⁸⁷I. Hwang, H. N. Kim, M. Seong, S. H. Lee, M. Kang, H. Yi, W. G. Bae, M. K. Kwak, and H. E. Jeong, *Adv. Healthcare Mater.* **7**, 1800275 (2018).
- ⁸⁸S. Baik, H. J. Lee, D. W. Kim, J. W. Kim, Y. Lee, and C. Pang, *Adv. Mater.* **31**, 1803309 (2019).
- ⁸⁹C. Li, R. Ye, J. Bouckaert, A. Zurutuza, D. Drider, T. Dumych, S. Paryzhak, V. Vovk, R. O. Bilyy, S. Melinte, M. Li, R. Boukherroub, and S. Szunerits, *ACS Appl. Mater. Interfaces* **9**, 36665 (2017).
- ⁹⁰X. He, S. Yang, C. Liu, T. Xu, and X. Zhang, *Adv. Healthcare Mater.* **9**, 2000941 (2020).
- ⁹¹L. Yang, K. Qi, L. Chang, A. Xu, Y. Hu, H. Zhai, and P. Lu, *J. Mater. Chem. B* **6**, 5031 (2018).
- ⁹²M. F. Farooqui and A. Shamim, *Sci. Rep.* **6**, 28949 (2016).
- ⁹³P. Mostafalu, W. Lenk, M. R. Dokmeci, B. Ziaie, A. Khademhosseini, and S. R. Sonkusale, *IEEE Trans. Biomed. Circuits Syst.* **9**, 670 (2015).
- ⁹⁴E. T. Hardy, Y. J. Wang, S. Iyer, R. G. Mannino, Y. Sakurai, T. H. Barker, T. Chi, Y. Youn, H. Wang, A. C. Brown, and W. A. Lam, *Lab Chip* **18**, 2985 (2018).
- ⁹⁵Y. Ogawa, K. Kato, T. Miyake, K. Nagamine, T. Ofuji, S. Yoshino, and M. Nishizawa, *Adv. Healthcare Mater.* **4**, 506 (2015).

- ⁹⁶A. J. Bandodkar, D. Molinuss, O. Mirza, T. Guinovart, J. R. Windmiller, G. Valdes-Ramirez, F. J. Andrade, M. J. Schoning, and J. Wang, *Biosens. Bioelectron.* **54**, 603 (2014).
- ⁹⁷T. Guinovart, A. J. Bandodkar, J. R. Windmiller, F. J. Andrade, and J. Wang, *Analyst* **138**, 7031 (2013).
- ⁹⁸J. R. Windmiller, A. J. Bandodkar, G. Valdes-Ramirez, S. Parkhomovsky, A. G. Martinez, and J. Wang, *Chem. Commun.* **48**, 6794 (2012).
- ⁹⁹A. J. Bandodkar, W. Jia, C. Yardimci, X. Wang, J. Ramirez, and J. Wang, *Anal. Chem.* **87**, 394 (2015).
- ¹⁰⁰W. Jia, A. J. Bandodkar, G. Valdes-Ramirez, J. R. Windmiller, Z. Yang, J. Ramirez, G. Chan, and J. Wang, *Anal. Chem.* **85**, 6553 (2013).
- ¹⁰¹W. Jia, G. Valdes-Ramirez, A. J. Bandodkar, J. R. Windmiller, and J. Wang, *Angew. Chem. Int. Ed.* **52**, 7233 (2013).
- ¹⁰²Y. J. Hong, H. Lee, J. Kim, M. Lee, H. J. Choi, T. Hyeon, and D.-H. Kim, *Adv. Funct. Mater.* **28**, 1805754 (2018).
- ¹⁰³C.-P. Chen, C.-Y. Chiang, Y.-Y. Yu, Y.-S. Hsiao, and W.-C. Chen, *Sol. Energy Mater. Sol. Cells* **165**, 111 (2017).
- ¹⁰⁴S. H. Kim, S. Jung, I. S. Yoon, C. Lee, Y. Oh, and J. M. Hong, *Adv. Mater.* **30**, 1800109 (2018).
- ¹⁰⁵J. Q. Zhang, Y. C. Wu, Z. Li, Y. C. Zhang, Y. Peng, D. Z. Chen, W. D. Zhu, S. R. Xu, C. F. Zhang, and Y. Hao, *Sci. Rep.* **9**, 15769 (2019).
- ¹⁰⁶H. Zhao, K. Li, M. Han, F. Zhu, A. Vazquez-Guardado, P. Guo, Z. Xie, Y. Park, L. Chen, X. Wang, H. Luan, Y. Yang, H. Wang, C. Liang, Y. Xue, R. D. Schaller, D. Chanda, Y. Huang, Y. Zhang, and J. A. Rogers, *Proc. Natl. Acad. Sci. U.S.A.* **116**, 13239 (2019).
- ¹⁰⁷Y. Wang, C. Zhao, J. Wang, X. Luo, L. Xie, S. Zhan, J. Kim, X. Wang, X. Liu, and Y. Ying, *Sci. Adv.* **7**, eabe4553 (2021).
- ¹⁰⁸J. Berry, *J. Mech. Phys. Solids* **8**, 194 (1960).
- ¹⁰⁹Z. Yan, T. Pan, M. Xue, C. Chen, Y. Cui, G. Yao, L. Huang, F. Liao, W. Jing, H. Zhang, M. Gao, D. Guo, Y. Xia, and Y. Lin, *Adv. Sci.* **4**, 1700251 (2017).
- ¹¹⁰H. L. Zhang, S. Feng, D. L. He, Y. G. Xu, M. H. Yang, and J. B. Bai, *Nano Energy* **48**, 256 (2018).
- ¹¹¹A. N. Abbas, B. Liu, L. Chen, Y. Ma, S. Cong, N. Aroonyadet, M. Kopf, T. Nilges, and C. Zhou, *ACS Nano* **9**, 5618 (2015).
- ¹¹²R. Soni, A. Raveendran, and S. Kurungot, *Nanoscale* **9**, 3593 (2017).
- ¹¹³W. Wang, K. Ouaras, A. L. Rutz, X. Li, M. Gerigk, T. E. Naegle, G. G. Malliaras, and Y. Y. S. Huang, *Sci. Adv.* **6**, eaba0931 (2020).
- ¹¹⁴J. Chen, Y. Huang, P. Kannan, L. Zhang, Z. Lin, J. Zhang, T. Chen, and L. Guo, *Anal. Chem.* **88**, 2149 (2016).
- ¹¹⁵M. Amjadi, A. Pichitpajongkit, S. Lee, S. Ryu, and I. Park, *ACS Nano* **8**, 5154 (2014).
- ¹¹⁶C. Pang, J. H. Koo, A. Nguyen, J. M. Caves, M. G. Kim, A. Chortos, K. Kim, P. J. Wang, J. B. Tok, and Z. Bao, *Adv. Mater.* **27**, 634 (2015).
- ¹¹⁷Y. Song, J. Min, Y. Yu, H. Wang, Y. Yang, H. Zhang, and W. Gao, *Sci. Adv.* **6**, eaay9842 (2020).
- ¹¹⁸Y. C. Shao, Q. Wang, Q. F. Dong, Y. B. Yuan, and J. S. Huang, *Nano Energy* **16**, 47 (2015).
- ¹¹⁹W. Honda, S. Harada, T. Arie, S. Akita, and K. Takei, *Adv. Funct. Mater.* **24**, 3299 (2014).
- ¹²⁰Y. Liu, C. Deng, D. Yi, X. Wang, Y. Tang, and Y. Wang, *Nanoscale* **9**, 15901 (2017).
- ¹²¹Q. Zhang, W. D. Jia, C. Ji, Z. Pei, Z. Jing, Y. Q. Cheng, W. D. Zhang, K. Zhuo, J. L. Ji, Z. Y. Yuan, and S. B. Sang, *Smart Mater. Struct.* **28**, 115040 (2019).
- ¹²²W. He, C. Wang, H. Wang, M. Jian, W. Lu, X. Liang, X. Zhang, F. Yang, and Y. Zhang, *Sci. Adv.* **5**, eaax0649 (2019).
- ¹²³V. De Zotti, K. Rapina, P. P. Cortet, L. Vanel, and S. Santucci, *Phys. Rev. Lett.* **122**, 068005 (2019).
- ¹²⁴H. T. Baytekin, B. Baytekin, and B. A. Grzybowski, *Angew. Chem. Int. Ed.* **51**, 3596 (2012).
- ¹²⁵T. Mazur and B. A. Grzybowski, *Chem. Sci.* **8**, 2025 (2017).
- ¹²⁶E. E. Donaldson, J. T. Dickinson, and X. A. Shen, *J. Adhes.* **19**, 267 (1986).
- ¹²⁷J. Horvat and R. A. Lewis, *Opt. Lett.* **34**, 2195 (2009).
- ¹²⁸E. N. Harvey, *Science* **89**, 460 (1939).
- ¹²⁹M. Zhenyi, F. Jiawen, and J. T. Dickinson, *J. Adhes.* **25**, 63 (2006).
- ¹³⁰D. Kramer, D. Lutzenkirchen-Hecht, B. Luhmann, K. Keite-Telgenbuscher, and R. Frahm, *Rev. Sci. Instrum.* **84**, 055104 (2013).
- ¹³¹H. Stocker, M. Ruhl, A. Heinrich, E. Mehner, and D. C. Meyer, *J. Electrostat.* **71**, 905 (2013).
- ¹³²E. Constable, J. Horvat, and R. A. Lewis, *Appl. Phys. Lett.* **97**, 131502 (2010).
- ¹³³A. J. Walton, *Adv. Phys.* **26**, 887 (1977).
- ¹³⁴C. Gay and L. Leibler, *Phys. Rev. Lett.* **82**, 936 (1999).
- ¹³⁵G. A. Mesyats, *Plasma Phys. Controlled Fusion* **47**, A109 (2005).
- ¹³⁶Z. L. Wang, *ACS Nano* **7**, 9533 (2013).
- ¹³⁷Y. Zi, H. Guo, Z. Wen, M.-H. Yeh, C. Hu, and Z. L. Wang, *ACS Nano* **10**, 4797 (2016).
- ¹³⁸B. Yang, W. Zeng, Z.-H. Peng, S.-R. Liu, K. Chen, and X.-M. Tao, *Adv. Energy Mater.* **6**, 1600505 (2016).
- ¹³⁹R. F. Frindt, *Phys. Rev. Lett.* **28**, 299 (1972).
- ¹⁴⁰M. Yi and Z. Shen, *J. Mater. Chem. A* **3**, 11700 (2015).
- ¹⁴¹R. Van Noorden, *Nature* **483**, 32 (2012).
- ¹⁴²K. S. Novoselov, D. Jiang, F. Schedin, T. J. Booth, V. V. Khotkevich, S. V. Morozov, and A. K. Geim, *Proc. Natl. Acad. Sci. U.S.A.* **102**, 10451 (2005).
- ¹⁴³H. Li, G. Lu, Y. Wang, Z. Yin, C. Cong, Q. He, L. Wang, F. Ding, T. Yu, and H. Zhang, *Small* **9**, 1974 (2013).
- ¹⁴⁴D. L. Duong, S. J. Yun, and Y. H. Lee, *ACS Nano* **11**, 11803 (2017).
- ¹⁴⁵J. Shim, S. H. Bae, W. Kong, D. Lee, K. Qiao, D. Nezich, Y. J. Park, R. K. Zhao, S. Sundaram, X. Li, H. Yeon, C. Choi, H. Kum, R. Y. Yue, G. Y. Zhou, Y. B. Ou, K. Lee, J. Moodera, X. H. Zhao, J. H. Ahn, C. Hinkle, A. Ougazzaden, and J. Kim, *Science* **362**, 665 (2018).
- ¹⁴⁶F. Liu, W. Wu, Y. Bai, S. H. Chae, Q. Li, J. Wang, J. Hone, and X. Y. Zhu, *Science* **367**, 903 (2020).
- ¹⁴⁷S. Cui, H. Pu, S. A. Wells, Z. Wen, S. Mao, J. Chang, M. C. Hersam, and J. Chen, *Nat. Commun.* **6**, 8632 (2015).
- ¹⁴⁸L. Li, Y. Yu, G. J. Ye, Q. Ge, X. Ou, H. Wu, D. Feng, X. H. Chen, and Y. Zhang, *Nat. Nanotechnol.* **9**, 372 (2014).
- ¹⁴⁹W. Bao, Z. Fang, J. Wan, J. Dai, H. Zhu, X. Han, X. Yang, C. Preston, and L. Hu, *ACS Nano* **8**, 10606 (2014).
- ¹⁵⁰C. Anichini, W. Czepa, D. Pakulski, A. Aliprandi, A. Ciesielski, and P. Samori, *Chem. Soc. Rev.* **47**, 4860 (2018).
- ¹⁵¹A. L. Friedman, F. K. Perkins, E. Cobas, G. G. Jernigan, P. M. Campbell, A. T. Hanbicki, and B. T. Jonker, *Solid-State Electron.* **101**, 2 (2014).
- ¹⁵²O. Lopez-Sanchez, D. Lembke, M. Kayci, A. Radenovic, and A. Kis, *Nat. Nanotechnol.* **8**, 497 (2013).
- ¹⁵³M. A. Krainak, X. Sun, G. Yang, and W. Lu, "Comparison of linear-mode avalanche photodiode lidar receivers for use at one-micron wavelength," *Proc. SPIE* **7681**, 76810Y (2010).
- ¹⁵⁴X. Wang, P. Wang, J. Wang, W. Hu, X. Zhou, N. Guo, H. Huang, S. Sun, H. Shen, T. Lin, M. Tang, L. Liao, A. Jiang, J. Sun, X. Meng, X. Chen, W. Lu, and J. Chu, *Adv. Mater.* **27**, 6575 (2015).
- ¹⁵⁵S. Chen, R. Cao, X. Chen, Q. Wu, Y. Zeng, S. Gao, Z. Guo, J. Zhao, M. Zhang, and H. Zhang, *Adv. Mater. Interfaces* **7**, 1902179 (2020).
- ¹⁵⁶Q. Zheng, J. Huang, S. Cao, and H. Gao, *J. Mater. Chem. C* **3**, 7469 (2015).
- ¹⁵⁷S. Kim, J. A. Wu, A. Carlson, S. H. Jin, A. Kovalsky, P. Glass, Z. J. Liu, N. Ahmed, S. L. Elgan, W. Q. Chen, P. M. Ferreira, M. Sitti, Y. G. Huang, and J. A. Rogers, *Proc. Natl. Acad. Sci. U.S.A.* **107**, 17095 (2010).
- ¹⁵⁸G. E. Bonacchini, C. Bossio, F. Greco, V. Mattoli, Y. H. Kim, G. Lanzani, and M. Caironi, *Adv. Mater.* **30**, 1706091 (2018).
- ¹⁵⁹J. L. Jiang, F. T. Zhao, S. W. Shi, Y. F. Du, J. Chen, S. F. Wang, J. S. Xu, C. M. Li, and J. S. Liao, *ACS Omega* **4**, 12319 (2019).
- ¹⁶⁰W. Mu, S. X. Sun, D. Jiang, Y. F. Fu, M. Edwards, Y. Zhang, K. Jeppson, and J. Liu, *J. Electron. Mater.* **44**, 2898 (2015).
- ¹⁶¹C. H. Deng, L. J. Pan, D. M. Zhang, C. W. Li, and H. Nasir, *Nanoscale* **9**, 16404 (2017).
- ¹⁶²C. C. Hsu, R. M. Chao, C. W. Liu, and S. Y. Liang, *J. Micromech. Microeng.* **21**, 075012 (2011).
- ¹⁶³Y. L. Tai and Z. G. Yang, *J. Mater. Chem. B* **3**, 5436 (2015).
- ¹⁶⁴J. W. Jeong, S. R. Yang, Y. H. Hur, S. W. Kim, K. M. Baek, S. Yim, H. I. Jang, J. H. Park, S. Y. Lee, C. O. Park, and Y. S. Jung, *Nat. Commun.* **5**, 5387 (2014).
- ¹⁶⁵X. Liu, J. Wang, L. Tang, L. Xie, and Y. Ying, *Adv. Funct. Mater.* **26**, 5515 (2016).
- ¹⁶⁶H. Yang, J. C. Love, F. Arias, and G. M. Whitesides, *Chem. Mater.* **14**, 1385 (2002).
- ¹⁶⁷S. H. Jeong, K. Hjort, and Z. Wu, *Sci. Rep.* **5**, 8419 (2015).

- ¹⁶⁸Q. X. Shang, W. Deng, X. J. Zhang, L. Wang, L. M. Huang, and J. S. Jie, *Adv. Electron. Mater.* **2**, 1600129 (2016).
- ¹⁶⁹Y. R. Tao, X. C. Wu, and W. W. Xiong, *Small* **10**, 4905 (2014).
- ¹⁷⁰A. Prabhakaran and P. Nayak, *ACS Appl. Nano Mater.* **3**, 391 (2020).
- ¹⁷¹X. Zang, C. Shen, E. Kao, R. Warren, R. Zhang, K. S. Teh, J. Zhong, M. Wei, B. Li, Y. Chu, M. Sanghadasa, A. Schwartzberg, and L. Lin, *Adv. Mater.* **30**, 1704754 (2018).
- ¹⁷²G. H. Li, B. L. Zhou, Z. Hou, Y. F. Wei, R. Wen, T. Ji, Y. Wei, Y.-Y. Hao, and Y.-X. Cui, *Nanoscale Research Letters* **17**, 8 (2022).
- ¹⁷³J. D. Caldwell, T. J. Anderson, J. C. Culbertson, G. G. Jernigan, K. D. Hobart, F. J. Kub, M. J. Tadjer, J. L. Tedesco, J. K. Hite, M. A. Mastro, R. L. Myers-Ward, C. R. Eddy, P. M. Campbell, and D. K. Gaskill, *ACS Nano* **4**, 1108 (2010).
- ¹⁷⁴S. B. Desai, S. R. Madhvapathy, M. Amani, D. Kiriya, M. Hettick, M. Tosun, Y. Zhou, M. Dubey, J. W. Ager III, D. Chrzan, and A. Javey, *Adv. Mater.* **28**, 4053 (2016).
- ¹⁷⁵Y. Lee, S. Bae, H. Jang, S. Jang, S. E. Zhu, S. H. Sim, Y. I. Song, B. H. Hong, and J. H. Ahn, *Nano Lett.* **10**, 490 (2010).
- ¹⁷⁶Y. R. Jeong, H. Park, S. W. Jin, S. Y. Hong, S.-S. Lee, and J. S. Ha, *Adv. Funct. Mater.* **25**, 4228 (2015).
- ¹⁷⁷X. Chen, H. R. Park, M. Pelton, X. Piao, N. C. Lindquist, H. Im, Y. J. Kim, J. S. Ahn, K. J. Ahn, N. Park, D. S. Kim, and S. H. Oh, *Nat. Commun.* **4**, 2361 (2013).
- ¹⁷⁸A. Cui, Z. Liu, H. L. Dong, F. X. Yang, Y. G. Zhen, W. X. Li, J. J. Li, C. Z. Gu, X. T. Zhang, R. J. Li, and W. P. Hu, *Adv. Mater.* **28**, 8227 (2016).
- ¹⁷⁹J. A. DeFranco, B. S. Schmidt, M. Lipson, and G. G. Malliaras, *Org. Electron.* **7**, 22 (2006).
- ¹⁸⁰R. S. Barnetson and L. J. Milne, *Br. J. Dermatol.* **88**, 487 (1973).
- ¹⁸¹D. Y. C. Fung, C. Y. Lee, and C. L. Kastner, *J. Food Prot.* **43**, 295 (1980).
- ¹⁸²B. Bisha and B. F. Brehm-Stecher, *Appl. Environ. Microbiol.* **75**, 1450 (2009).
- ¹⁸³S. Darvishi, H. Pick, T. E. Lin, Y. D. Zhu, X. Y. Li, P. C. Ho, H. H. Girault, and A. Lesch, *Anal. Chem.* **91**, 12900 (2019).
- ¹⁸⁴W. Wachsmann, V. Morhenn, T. Palmer, L. Walls, T. Hata, J. Zalla, R. Scheinberg, H. Sofen, S. Mraz, K. Gross, H. Rabinovitz, D. Polsky, and S. Chang, *Br. J. Dermatol.* **164**, 797 (2011).
- ¹⁸⁵D. Wang, F. Wang, and H. Yang, *Sens. Actuators, B* **274**, 676 (2018).
- ¹⁸⁶Z. Liu, L. Cheng, L. Zhang, C. Jing, X. Shi, Z. Yang, Y. Long, and J. Fang, *Nanoscale* **6**, 2567 (2014).
- ¹⁸⁷D. Li, L. Tang, J. Wang, X. Liu, and Y. Ying, *Adv. Opt. Mater.* **4**, 1475 (2016).
- ¹⁸⁸A. Korkmaz, M. Kenton, G. Aksin, M. Kahraman, and S. Wachsmann-Hogiu, *ACS Appl. Nano Mater.* **1**, 5316 (2018).
- ¹⁸⁹Y. Zhu, M. Li, D. Yu, and L. Yang, *Talanta* **128**, 117 (2014).
- ¹⁹⁰Y. Dai, H. Hu, M. Wang, J. Xu, and S. Wang, *Nat. Electron.* **4**, 17 (2021).
- ¹⁹¹H. Chen, Y. Xu, L. Bai, Y. Jiang, J. Zhang, C. Zhao, T. Li, H. Yu, G. Song, N. Zhang, and Q. Gan, *Adv. Mater. Technol.* **2**, 1700044 (2017).
- ¹⁹²Y. L. Tai and Z. G. Yang, *Adv. Mater. Interfaces* **4**, 1700496 (2017).
- ¹⁹³M. Fu, J. Zhang, Y. Jin, Y. Zhao, S. Huang, and C. F. Guo, *Adv. Sci.* **7**, 2000258 (2020).
- ¹⁹⁴L. W. Lo, H. Y. Shi, H. C. Wan, Z. H. Xu, X. B. Tan, and C. Wang, *Adv. Mater. Technol.* **5**, 1900717 (2020).
- ¹⁹⁵B. Li, M. R. Wang, R. Subair, G. Z. Cao, and J. J. Tian, *J. Phys. Chem. C* **122**, 25260 (2018).
- ¹⁹⁶L. Teng, L. F. Zhu, S. Handschuh-Wang, and X. C. Zhou, *J. Mater. Chem. C* **7**, 15243 (2019).
- ¹⁹⁷A. W. Martinez, S. T. Phillips, and G. M. Whitesides, *Proc. Natl. Acad. Sci. U.S.A.* **105**, 19606 (2008).
- ¹⁹⁸H. Lee, C. Song, Y. S. Hong, M. S. Kim, H. R. Cho, T. Kang, K. Shin, S. H. Choi, T. Hyeon, and D. H. Kim, *Sci. Adv.* **3**, e1601314 (2017).
- ¹⁹⁹M. N. Pastore, Y. N. Kalia, M. Horstmann, and M. S. Roberts, *Br. J. Pharmacol.* **172**, 2179 (2015).
- ²⁰⁰X. He, T. Xu, Z. Gu, W. Gao, L. P. Xu, T. Pan, and X. Zhang, *Anal. Chem.* **91**, 4296 (2019).
- ²⁰¹W. Gao, S. Emaminejad, H. Y. Y. Nyein, S. Challa, K. Chen, A. Peck, H. M. Fahad, H. Ota, H. Shiraki, D. Kiriya, D. H. Lien, G. A. Brooks, R. W. Davis, and A. Javey, *Nature* **529**, 509 (2016).
- ²⁰²M. Bariya, H. Y. Y. Nyein, and A. Javey, *Nat. Electron.* **1**, 160 (2018).
- ²⁰³X. He, C. Fan, T. Xu, and X. Zhang, *Nano Lett.* **21**, 8880 (2021).
- ²⁰⁴J. T. Reeder, Y. Xue, D. Franklin, Y. Deng, J. Choi, O. Prado, R. Kim, C. Liu, J. Hanson, J. Ciraldo, A. J. Bandodkar, S. Krishnan, A. Johnson, E. Patnaude, R. Avila, Y. Huang, and J. A. Rogers, *Nat. Commun.* **10**, 5513 (2019).
- ²⁰⁵A. J. Bandodkar, P. Gutruf, J. Choi, K. Lee, Y. Sekine, J. T. Reeder, W. J. Jeang, A. J. Aranyosi, S. P. Lee, J. B. Model, R. Ghaffari, C. J. Su, J. P. Leshock, T. Ray, A. Verrillo, K. Thomas, V. Krishnamurthi, S. Han, J. Kim, S. Krishnan, T. Hang, and J. A. Rogers, *Sci. Adv.* **5**, eaav3294 (2019).
- ²⁰⁶J. Xiao, Y. Liu, L. Su, D. Zhao, L. Zhao, and X. Zhang, *Anal. Chem.* **91**, 14803 (2019).
- ²⁰⁷H. Lee, T. K. Choi, Y. B. Lee, H. R. Cho, R. Ghaffari, L. Wang, H. J. Choi, T. D. Chung, N. Lu, T. Hyeon, S. H. Choi, and D. H. Kim, *Nat. Nanotechnol.* **11**, 566 (2016).
- ²⁰⁸B. Ketelsen, M. Yesilmen, H. Schlicke, H. Noei, C. H. Su, Y. C. Liao, and T. Vossmeier, *ACS Appl. Mater. Interfaces* **10**, 37374 (2018).
- ²⁰⁹X. He, Q. Pei, T. Xu, and X. Zhang, *Sens. Actuators, B* **304**, 127415 (2020).
- ²¹⁰X. He, T. Xu, W. Gao, L. P. Xu, T. Pan, and X. Zhang, *Anal. Chem.* **90**, 14105 (2018).
- ²¹¹H. Posada-Quintero, R. Rood, K. Burnham, J. Pennace, and K. Chon, *IEEE J. Transl. Eng. Health Med.* **4**, 2100209 (2016).
- ²¹²W. Jo, K. Jeong, Y.-S. Park, J.-I. Lee, S. Gap Im, and T.-S. Kim, *Chem. Eng. J.* **452**, 139050 (2023).
- ²¹³W. Kim, I. Lee, D. Yoon Kim, Y. Y. Yu, H. Y. Jung, S. Kwon, W. Seo Park, and T. S. Kim, *Nanotechnology* **28**, 194002 (2017).
- ²¹⁴B. Ciui, A. Martin, R. K. Mishra, B. Brunetti, T. Nakagawa, T. J. Dawkins, M. Lyu, C. Cristea, R. Sandulescu, and J. Wang, *Adv. Healthcare Mater.* **7**, 1701264 (2018).
- ²¹⁵J. Li, S. Sollami Delekta, P. Zhang, S. Yang, M. R. Lohe, X. Zhuang, X. Feng, and M. Ostling, *ACS Nano* **11**, 8249 (2017).
- ²¹⁶W. Wang, H. Bai, H. Y. Li, Q. Lv, Q. Zhang, and N. Bao, *Sens. Actuators, B* **236**, 218 (2016).
- ²¹⁷V. Sanchez-Romaguera, M. A. Ziai, D. Oyeka, S. Barbosa, J. S. R. Wheeler, J. C. Batchelor, E. A. Parker, and S. G. Yeates, *J. Mater. Chem. C* **1**, 6395 (2013).
- ²¹⁸I. M. Asuo, P. Fourmont, I. Ka, D. Gedamu, S. Bouzidi, A. Pignolet, R. Nechache, and S. G. Cloutier, *Small* **15**, 1804150 (2019).
- ²¹⁹K. M. Frazier, K. A. Mirica, J. J. Walsh, and T. M. Swager, *Lab Chip* **14**, 4059 (2014).
- ²²⁰J. Smith and H. Arnolds, *J. Raman Spectrosc.* **49**, 1236 (2018).
- ²²¹M. M. Song, L. T. Dang, J. Long, and C. G. Hu, *ACS Sens.* **3**, 2518 (2018).
- ²²²L. Zhao, T. Guo, L. Wang, Y. Liu, G. Chen, H. Zhou, and M. Zhang, *Anal. Chem.* **90**, 777 (2018).
- ²²³C. G. Li, H.-A. Joung, H. Noh, M.-B. Song, M.-G. Kim, and H. Jung, *Lab Chip* **15**, 3286 (2015).
- ²²⁴A. Fraiwan, S. Mukherjee, S. Sundermier, H. S. Lee, and S. Choi, *Biosens. Bioelectron.* **49**, 410 (2013).
- ²²⁵H. Wang, S. Li, Y. Wang, H. Wang, X. Shen, M. Zhang, H. Lu, M. He, and Y. Zhang, *Adv. Mater.* **32**, 1908214 (2020).
- ²²⁶C. Damm and W. Peukert, *Langmuir* **25**, 2264 (2009).
- ²²⁷B. Baytekin, H. T. Baytekin, and B. A. Grzybowski, *J. Am. Chem. Soc.* **134**, 7223 (2012).
- ²²⁸I. S. Lee, Y. J. Tak, B. H. Kang, H. Yoo, S. Jung, and H. J. Kim, *ACS Appl. Mater. Interfaces* **12**, 19123 (2020).
- ²²⁹H. Lee, T. S. Jung, J. W. Park, and H. J. Kim, *ACS Appl. Mater. Interfaces* **10**, 37216 (2018).
- ²³⁰W. Deng, L. Jin, B. Zhang, Y. Chen, L. Mao, H. Zhang, and W. Yang, *Nanoscale* **8**, 16302 (2016).
- ²³¹Y. Wang, L. Zhao, Y. Zhao, W. Y. Wang, Y. Liu, C. Gu, J. Li, G. Zhang, T. J. Huang, and S. Yang, *Adv. Mater.* **30**, 1870395 (2018).
- ²³²J. Li, A. D. Celiz, J. Yang, Q. Yang, I. Wamala, W. Whyte, B. R. Seo, N. V. Vasilyev, J. J. Vlassak, Z. Suo, and D. J. Mooney, *Science* **357**, 378 (2017).
- ²³³D. H. Kim, J. Vientti, J. J. Amsden, J. Xiao, L. Vigeland, Y. S. Kim, J. A. Blanco, B. Panilaitis, E. S. Frechette, D. Contreras, D. L. Kaplan, F. G. Omenetto, Y. Huang, K. C. Hwang, M. R. Zakin, B. Litt, and J. A. Rogers, *Nat. Mater.* **9**, 511 (2010).
- ²³⁴D. H. Kim, Y. S. Kim, J. Amsden, B. Panilaitis, D. L. Kaplan, F. G. Omenetto, M. R. Zakin, and J. A. Rogers, *Appl. Phys. Lett.* **95**, 133701 (2009).
- ²³⁵S. B. Bon, I. Chiesa, M. Degli Esposti, D. Morselli, P. Fabbri, C. De Maria, A. Morabito, R. Coletta, M. Calamai, F. S. Pavone, R. Tonin, A. Morrone, G. Giorgi, and L. Valentini, *ACS Appl. Mater. Interfaces* **13**, 21007 (2021).